

AD A090796

LEVEL II

①

THREE-DIMENSIONAL RESPONSE OF AN AUTOMOBILE  
TO A GENERALIZED IMPULSE

A Thesis

by

JOHN FREDERICK BETZ

DTIC  
ACTE  
OCT 24 1980  
E

Submitted to the Graduate College of  
Texas A&M University  
in partial fulfillment of the requirement for the degree of  
MASTER OF SCIENCE

December 1979

Major Subject: Civil Engineering

DISTRIBUTION STATEMENT A  
Approved for public release;  
Distribution Unlimited

80 10 14 232

UNCLASS

SECURITY CLASSIFICATION OF THIS PAGE (When Data Entered)

14 AFIT 7-CI-REPORT DOCUMENTATION PAGE		READ INSTRUCTIONS BEFORE COMPLETING FORM
1. REPORT NUMBER 79-245T	2. GOVT ACCESSION NO. AD-A090	3. RECIPIENT'S CATALOG NUMBER 796
4. TITLE (and Subtitle) Three-Dimensional Response of an Automobile to a Generalized Impulse		5. TYPE OF REPORT & PERIOD COVERED THESIS/DISSERTATION
7. AUTHOR(s) John Frederick Betz		6. PERFORMING ORG. REPORT NUMBER
9. PERFORMING ORGANIZATION NAME AND ADDRESS AFIT STUDENT AT: Texas A&M University		8. CONTRACT OR GRANT NUMBER(s)
11. CONTROLLING OFFICE NAME AND ADDRESS AFIT/NR WPAFB OH 45433		10. PROGRAM ELEMENT, PROJECT, TASK AREA & WORK UNIT NUMBERS
14. MONITORING AGENCY NAME & ADDRESS (if different from Controlling Office)		12. REPORT DATE Dec 79
15. SECURITY CLASS. (of this report) UNCLASS		13. NUMBER OF PAGES 101
16. DISTRIBUTION STATEMENT (of this Report) APPROVED FOR PUBLIC RELEASE; DISTRIBUTION UNLIMITED		15a. DECLASSIFICATION/DOWNGRADING SCHEDULE
17. DISTRIBUTION STATEMENT (of the abstract entered in Block 20, if different from Report)		
18. SUPPLEMENTARY NOTES APPROVED FOR PUBLIC RELEASE: IAW AFR 190-17 35 SEP 1980		Fredric C. Lynch FREDRIC C. LYNCH, Major, USAF Director of Public Affairs Air Force Institute of Technology (ATC) Wright-Patterson AFB, OH 45433
19. KEY WORDS (Continue on reverse side if necessary and identify by block number)		
20. ABSTRACT (Continue on reverse side if necessary and identify by block number)  ATTACHED		

80 10 14 232

THREE-DIMENSIONAL RESPONSE OF AN AUTOMOBILE  
TO A GENERALIZED IMPULSE

A Thesis

by

JOHN FREDERICK BETZ

Submitted to the Graduate College of  
Texas A&M University  
in partial fulfillment of the requirement for the degree of  
MASTER OF SCIENCE

December 1979

Major Subject: Civil Engineering

Accession For	
NTIS - GEMRI	<input checked="" type="checkbox"/>
DDC TAB	<input type="checkbox"/>
Unannounced	<input type="checkbox"/>
Justification	<input type="checkbox"/>
By _____	
Distribution / _____	
Special Handling / _____	
Dist.	Acquisition For Special
<b>A</b>	

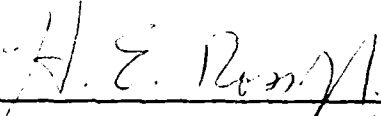
THREE-DIMENSIONAL RESPONSE OF AN AUTOMOBILE  
TO A GENERALIZED IMPULSE

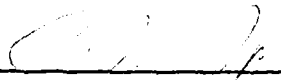
A Thesis

by

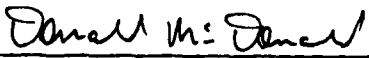
JOHN FREDERICK BETZ

Approved as to style and content by:

  
\_\_\_\_\_  
(Chairman of Committee)

  
\_\_\_\_\_  
(Member)

  
\_\_\_\_\_  
(Member)

  
\_\_\_\_\_  
(Head of Department)

## ABSTRACT

Three-Dimensional Response of an Automobile to  
a Generalized Impulse. (December 1979)

John Frederick Betz, B.S., United States Air Force Academy

Chairman of Advisory Committee: Dr. Hayes E. Ross, Jr.

↙  
Roadside design standards have not kept pace with the recent upswing of compact and subcompact vehicle traffic on the highways. Written when the predominant vehicle size was larger than the present trends, these standards require examination in light of the smaller, lighter vehicles. By modifying the highway-vehicle-object simulation model (HVOSM) (9), a three-dimensional computer simulation of signpost impacts is available as a tool to evaluate the standards.

In the course of this thesis, validation of the modified HVOSM was completed to prove the reliability of the program in simulating real collisions; then, the parameter studies were carried out. Signpost models meeting the upper limits of the AASHTO standards (10) were prepared. The two models represented the major signpost installation methods: a breakaway signpost connected to a base at ground level, and a base-bending signpost placed directly into the ground. Then, large, medium, compact and subcompact vehicle impacts with the signpost models were simulated using the modified HVOSM.

In each case, the subcompact vehicle experiences extreme accelerations and total loss of control. The breakaway sign model causes spinout of the subcompact car, while the base-bending model impact results in vehicle rollover. Each study reveals the anticipated

results: the occupants of the two larger vehicles survive impact in a stable, safe fashion, while the two smaller cars, especially the sub-compact, experience hazardous accelerations and vehicle instability after impact. These results all point to a re-evaluation of roadside design standards as presented by AASHTO.

## ACKNOWLEDGMENTS

The author is indebted to Darrell G. Smith and Dale L. Shafer, without whose direction and timely suggestions the computer program would never have been repaired so that the new computer would accept it. The help of Kenneth C. Walker in parts of the validation effort is appreciated, as is the able drafting ability of Michael Byrd. The lightning precision of Sylvia Velasco in typing this thesis is also highly appreciated.

This paper was made possible by the support of the Fannie and John Hertz Foundation. The author is thankful for their interest and backing. The support of TTI in funding the computer work, typing, drafting, and copying costs is greatly appreciated.

Finally, the efforts of the thesis committee in helping the author present a valid and organized presentation are highly esteemed. Dr. H. E. Ross, Jr., Dr. T. J. Hirsch, and Dr. C. M. Hix all provided guidance both through course work and advisory roles for this thesis.

## TABLE OF CONTENTS

	<u>Page</u>	
I	PROBLEM BACKGROUND	1
	Introduction	1
	Program Selection	2
	Decision	4
II	PROGRAM MODIFICATION	5
	Background	5
	Input Phase	5
	Mathematical Operations	11
	Output Phase	14
	Conclusion	16
III	PROGRAM VALIDATION	17
	General Approach	17
	Linear Deceleration	18
	LaGrangian Analysis	20
	Crash Test Number 11	29
	Crash Test Number 9	31
	Conclusion	38
IV	PARAMETER STUDY APPLICATION	39
	Introduction	39
	Signpost Models	39
	Vehicle Data	42
	Conclusion	51
V	PARAMETER STUDY RESULTS	52
	Introduction	52



## TABLE OF CONTENTS (continued)

	<u>Page</u>
Longitudinal Acceleration	53
Vertical Acceleration	60
Travel Path	67
Summary	79
VI CONCLUSION	81
APPENDICES	
I REFERENCES	83
II A DESCRIPTION OF THE HIGHWAY-VEHICLE-OBJECT SIMULATION MODEL	84
III CORRECTION OF ORIGINAL HVOSM FOR IBM 360 COMPUTER AND CURRENT FORTRAN H EXTENDED COMPILER	87
IV PROGRAM MODIFICATION LISTING	95

LIST OF TABLES

1.	Crash Test #11 Duplication	33
2.	Crash Test #9 Duplication	33
3.	Vehicle Sign Impact Results	80

## LIST OF FIGURES

1.	Linear Deceleration Test	19
2.	LaGrangian Coordinate Systems	21
3.	Velocity of Vehicle in Local X Direction	25
4.	Velocity of Vehicle in Local Y Direction	26
5.	Vehicle Location Along Global X Axis	27
6.	Vehicle Yaw Speed	28
7.	Input for Crash Test Comparisons	30
8.	Vertical Impulse Input for Crash Test #11 Duplication	32
9.	Right Accelerometer Readouts	34
10.	Vertical Impulse Input for Crash Test #9 Duplication	36
11.	Left Accelerometer Readouts	37
12.	Horizontal Impulse Input for All Cars	41
13.	Vertical Impulse Input for All Cars	43
14.	Input for Large Car	46
15.	Input for Medium Car	47
16.	Input for Compact Car	49
17.	Input for Subcompact Car	50
18.	Sprung Mass C.G. Longitudinal Acceleration for Large Car	54
19.	Sprung Mass C.G. Longitudinal Acceleration for Medium Car	55
20.	Sprung Mass C.G. Longitudinal Acceleration for Compact Car	57
21.	Sprung Mass C.G. Longitudinal Acceleration for Subcompact Car	58

## LIST OF FIGURES (continued)

22.	Sprung Mass C.G. Vertical Acceleration for Large Car in Base-Bending Model	61
23.	Sprung Mass C.G. Vertical Acceleration for Medium Car in Base-Bending Model	63
24.	Sprung Mass C.G. Vertical Acceleration for Compact Car in Base-Bending Model	64
25.	Sprung Mass C.G. Vertical Acceleration for Subcompact Car	66
26.	Path and Orientation of Large Car in Breakaway Model	68
27.	Path and Orientation of Large Car in Base-Bending Model	70
28.	Path and Orientation of Medium Car in Breakaway Model	71
29.	Path and Orientation of Medium Car in Base-Bending Model	72
30.	Path and Orientation of Compact Car in Breakaway Model	74
31.	Path and Orientation of Compact Car in Base-Bending Model	75
32.	Path and Orientation of Subcompact Car in Breakaway Model	77
33.	Path and Orientation of Subcompact Car in Base-Bending Model	78
34.	Idealization of Automobile	85
35.	Modification of MAIN Program	96
36.	Modification of INPUT Subroutine	97
37.	Modification of SFORCE Subroutine	100

LIST OF FIGURES (continued)

38.	Modification of IDOUT Subroutine	101
-----	----------------------------------	-----

CHAPTER I  
PROBLEM BACKGROUND

Introduction

A quick inspection of current attitudes and changing lifestyles is very revealing about the trend in size today. The concept of "the boys want less" is even carried into the automobile market, where the rising prices and concurrent shortages of gasoline have combined to make the large, old-fashioned status symbol obsolete. Cars labeled as "gas-guzzlers" are avoided, and the newer cars are much smaller and lighter to meet the increasing demand for higher range and gas mileage.

The national highway standards, however, do not reflect these changes. Although any changes in national standards should not be made to reflect mere trends, a quick examination of Europe, where gasoline has been high-priced for some time, indicates that the smaller cars will become a larger proportion of traffic in the future.

The signposts and light poles along the highways in the U.S. have been designed using existing AASHTO specifications (10), which were developed for compact sized (2250 pounds) automobiles. The present car size trend, however, includes many subcompact cars weighing 1800 pounds or less. This is one factor which indicates the need for a re-examination of the AASHTO standards.

Testing performed by the Texas Transportation Institute (TTI) (7) also presented some interesting information to substantiate the need

---

The model journal chosen for this thesis was the Journal of the Engineering Mechanics Division, Proceedings of the American Society of Civil Engineers.

for re-evaluation. These tests were originally performed to test the effects of different signpost configurations on Chevrolet Vegas, a compact car, in simulated impacts. An interesting development in the tests was that the Vega came quite close to rollover in several of the impacts. The vehicle actually did experience rollover in one test (test #11), but the sign configuration did not meet existing AASHTO standards. However, the important fact was that the rollover was nearly the result in several collisions with signs that met the standards. Smaller cars are more likely to experience rollover than larger cars, so it is quite possible that subcompact cars would have actually rolled over in the same situations. This second factor, the near rollover of compact cars in impacts with signposts meeting AASHTO standards, combined with the car size trend toward smaller and lighter automobiles, formed the basis for this thesis.

The concern of this thesis is then the examination of signpost impacts using computer simulation. The behavior of subcompact, compact, medium, and large cars in collisions with a signpost or light pole meeting AASHTO design criteria will be studied to reveal whether the existing standards allow rollover to occur in the smaller automobiles.

#### Program Selection

Two existing computer simulations of automobiles were examined to determine which was better suited to study signpost impacts. These programs were the Highway-Vehicle-Object Simulation Model (HVOSM) (8) and the Simulation Model of Automobile Collisions (SMAC) (4). Each one had negative and positive aspects which were examined in light of the

requirements of the planned simulations. The final choice turned out to be much easier than anticipated due to the strong negative aspects of one of the programs.

The HVOSM was developed to simulate the three-dimensional motion of an automobile subjected to roadside guardrail collisions or a run-off-road accident. It was also developed to study the ride and handling behavior of an automobile traversing a given roadway configuration. The program has been effectively used in guardrail evaluations and roadside design for several years. The shortcoming of the current program is in the lack of provisions to simulate impacts of the model vehicle with roadway signs or lampposts. Thus, if this program were to be used in this study, extensive modifications would be required to add impulse evaluation to the possible program functions. However, the program has the advantages of three-dimensional motion and proven performance in the design of highways and roadside structures.

SMAC is another computer program, and it is used to evaluate impacts between automobiles and signposts. SMAC was originally developed by Calspan and further modified by TTI. Despite the fact that the program was developed to study signpost impacts, there are two inherent weaknesses in the program which invalidate its use in this study. First of all, the program only considers two-dimensional (planar) motion. Since this study is concerned with possible vehicle rollover, a planar model of collision is unsuitable. Finally, the program assumes that the signposts are perfectly rigid. Breakaway posts are designed to prevent the negative aspects of rigidity, and nonbreakaway posts create



large downward forces on automobiles when the signposts plastically deform and wrap around the car frame as the vehicle rides them down. Since the SMAC model does not consider the three-dimensional motion required for rollover and it evaluates only rigid posts in collisions, the SMAC model is unsuited for this study. The modification required for the SMAC model would amount to changing the entire program, which would be a greater task than modifying the HVOSM.

#### Decision

An analysis of the features of the HVOSM and the SMAC programs resulted in the choice of the HVOSM as the program best suited for this study. Modifications had to be made to the HVOSM to allow the option of accepting generalized impulse data to simulate signpost impacts. The program was to simulate the effects of any general force acting on any location of the vehicle. Since any general force can be broken down into its components aligned with the vehicle axes, the program would use the time-dependent force and location data as referenced to and oriented with the principle vehicle axes. The location data would locate the point of the force application from the sprung mass center of gravity of the vehicle measured along those axes. The implementation of these modifications to the HVOSM is the subject of the next chapter. Further references and a figure relating to the HVOSM can be found in Appendix II.

## CHAPTER II PROGRAM MODIFICATION

### Background

As previously mentioned, the HVOSM is a proven program of numerous capabilities. Mainly used for roadside barrier design and studies of automobile behavior on varying surfaces, the program had to be modified to accept new options without interfering with its existing abilities. After correcting the errors due to differences in the compilers (Appendix III), the program was studied at length to insure that the changes were made to affect the fewest subroutines and therefore minimize any possible errors. The changes themselves were quite simple, and the whole series of modifications was simply a matter of finding where the critical operations took place.

The changes, and thus the divisions of this chapter, can be classed into three areas: the input phase, the mathematical operations, and the output phase. The actual computer listings of the changes as they appear in the program can be found in Appendix IV. The theory and implementation of the changes are the subject of the divisions in this chapter.

### Input Phase

The HVOSM had to be modified to accept a new matrix of time-dependent force and location data. Fifty time points were considered to be adequate to describe a sign impact with the use of linear interpolation between time points. Since the matrix had to define the

time, the forces in the three principal directions, and the three-dimensional location of the point of application, the matrix was sized as 7 by 50. Another necessary pair of additions were a variable that could be used to trigger the sign impact program option into operation, and a variable to define the total number of time points used for each problem (since fifty time points would not always be necessary).

As each of these new variables were to be used in a number of subroutines, they were added to existing common blocks in the program rather than adding to the argument of the individual subroutine. The variables were named as follows: The time, force, and location matrix was named SUBB(7,50); the sign impact option trigger was named COLL; and the variable for the number of time points was named NUMT (an integer-valued variable). The SUBB matrix and the COLL variable were then added to the end of the BARIER common block throughout the program, and the NUMT variable was added to the INPT1 common block throughout the program. The initial values of these values were all cleared to zero in the initial part of the main program. COLL and the SUBB matrix were cleared along with the rest of the BARIER common block using the ERASE subroutine, while NUMT was cleared to zero by adding a simple program statement.

After the variables were set up and ready to accept the proper numbers, the actual input operation was next completed. This involved modifying the INPUT subroutine to accept the additional values. In the HVOSM, the input is organized according to ICARD values which are specified by a number in columns 79 and 80 on the input data cards. The ICARD values are used to specify a GO TO statement location in the

INPUT subroutine, where the values from the cards are affixed to the proper variables. The cards are divided into fields of eight characters each, with nine fields per card. Thus, some ICARD values did not use the full allotment of nine fields, and these unused fields could be used to define the COLL and NUMT variable values. The great size of SUBB matrix warranted creation of a new ICARD series to transfer the matrix values.

A further explanation of the workings of the INPUT subroutine will help to ease the explanation of the changes performed on the subroutine to load these variables. The subroutine reads the data cards and records them in card images which are then printed in the output phase so that the values as the computer reads them can be checked for error. However, those same values, which are contained in nine fields of eight characters each, are loaded into nine locations in a temporary one-dimensional matrix named DUM(9). The values from each of the nine fields are loaded into DUM(1) through DUM(9), respectively. Then, the GO TO statement, keyed by the ICARD value, leads the program to the correct section, where those values are loaded from the DUM matrix into the corresponding program variables. If an ICARD series does not use the full nine fields, then some of the DUM matrix locations are not utilized and these openings are available for variable additions without changing the program (other than the required variable loading statements with the unused matrix locations).

The ICARD=2 data set only used seven of the nine fields on the data card, so the eighth and ninth fields on that card were used to define COLL and NUMT, respectively. Then, since the ICARD=2 value

sends control to statement number 4 in the INPUT subroutine, the statements

COLL = DUM(8)

NUMT = DUM(9)

were added after the statement assigning the DUM(7) value to a variable name. Thus, simply by using the full capabilities of the ICARD=2 data set, COLL and NUMT input values were added to the program with only two program statements.

The SUBB matrix presented a greater challenge. First of all, each of the matrix locations had to be defined for the proper input alignment. The locations of the SUBB(7,50) matrix were defined as follows, using the general location SUBB(A,B):

1. All A=1 locations are discrete time values, in seconds.
2. All A=2 locations are instantaneous force magnitudes aligned with the local vehicle x-axis, in pounds (+ or -).
3. All A=3 locations are instantaneous force magnitudes aligned with the local vehicle y-axis, in pounds (+ or -).
4. All A=4 locations are instantaneous force magnitudes aligned with the local vehicle z-axis, in pounds (+ or -).
5. All A=5 locations are the distance from the sprung mass center of gravity to the point of force application measured along the vehicle x-axis, in inches (+ or -).
6. All A=6 locations are the distance from the sprung mass center of gravity to the point of force application measured along the vehicle y-axis, in inches (+ or -).
7. All A=7 locations are the distance from the sprung mass center

of gravity to the point of force application measured along the vehicle z-axis, in inches (+ or -).

8. All B values, from a minimum of 2 up to a possible 50, are the values of each set of forces and locations corresponding to each discrete time value.

As can be seen from the definitions listed above, the forces all act at a point for each time value.

Next, the ICARD=29 provision (the last program data set ICARD value had been 28) had to be added to the GO TO statement, using the statement number chosen for the additional data set. Statement number 53 was not in use elsewhere in the INPUT subroutine, so it was used to locate the ICARD=29 variable loading statements. After adding location 53 to the GO TO argument, statement number 53 and the rest of the ICARD=29 variable loading statements were inserted directly between the next-to-last statement and the END statement in the INPUT subroutine.

All that remained was to add the statements to transfer the values from the DUM matrix positions to the proper locations in the SUBB matrix. An additional counter variable was added for this purpose. The variable JJ was set equal to zero at the start of the program with an additional statement. JJ defines the location of each set of data for each time set, thereby sequentially loading the seven variables into the SUBB matrix. This requires that the ICARD=29 data deck be organized in order of increasing time values, both for this sequential loading and for use in linear interpolation later in the program. It is vitally important to the operation of the program that the data cards be in order of sequentially increasing time values.

After defining the SUBB matrix and inserting JJ as a counter variable, the following statements were added to complete the input of the SUBB matrix:

```
53  JJ = JJ+1
      SUBB(1, JJ) = DUM(1)
      SUBB(2, JJ) = DUM(2)
      SUBB(3, JJ) = DUM(3)
      SUBB(4, JJ) = DUM(4)
      SUBB(5, JJ) = DUM(5)
      SUBB(6, JJ) = DUM(6)
      SUBB(7, JJ) = DUM(7)
      GO TO 2
```

Therefore, the data card only uses seven of the nine fields provided, and the variables are loaded in the order of time, x, y, and z forces, and the x, y, and z locations.

That was the extent of the necessary modifications to input the values for the sign impact option. The important changes to remember to operate the sign impact option are that COLL and NUMT are the eighth and ninth variables on the ICARD=2 data set, where COLL is input as 1.0 to trigger the sign impact option and NUMT is set equal to the number of discrete time points used in the SUBB matrix to define the impulse input. Also, the ICARD=29 data set, which must be entered in the order of sequentially increasing time steps, is used to load the SUBB matrix. The first seven fields are used, defined as the time (in seconds), the x, y, and z forces (in pounds), and the x, y, and z locations (in inches), respectively, in the first through seventh fields.

Important requirements are that the first time step should always be zero, and the last time step should be set after the program is anticipated to stop running. In other words, if the program is set to investigate only the first 3 seconds of car motion, then the last time step should be set to greater than 3 seconds for proper program operation.

#### Mathematical Operations

After the time, force, and location data and the trigger variable were input to the program, the next obstacle was to find exactly where in the program to insert the equations used to compute the forces and moments acting on the automobile during sign impact. A thorough analysis of the program provided the location which required relatively few additions to the program to add the necessary equations.

The SFORCE subroutine, with the help of several subordinate subroutines, calculates the forces and moments acting on the vehicle due to roadside guardrail collisions. SFORCE calls several subordinate subroutines in the course of its operation, most notably RESFRC, which uses the information developed in the SFORCE subroutine to compute the forces and moments acting on the automobile.

Since all these operations could be narrowed down to the SFORCE subroutine, the sign impact modifications were placed at the tail end of the subroutine, and the COLL trigger was placed to circumvent the normal operation of SFORCE and the subordinate subroutine. As all the collision forces and moments used by the HVOSM originated in the SFORCE subroutine and its subordinate subroutines, the addition of the signpost impact option trigger and the correct equations, using the



same variable names used by the RESFRC subroutine, to the SFORCE subroutine were the only necessary program modifications for the mathematical operations.

First of all, the SFORCE subroutine sign impact option trigger statement had to be set up and placed before the first operational subroutine statements. The COLL variable was used in its trigger function at the head of the program, directly following the clearing of the variables (when they are set equal to zero). The statement added was

```
IF(COLL.EQ.1.) GO TO 1002
```

where 1002 is the statement number of the first of the sign impact modification option statements. As defined in the input phase, COLL is set equal to 1.0 to trigger the sign impact option in the ICARD=2 data set.

Finally, the statements for the mathematical operations had to be organized and placed starting at statement number 1002. Also, the program variables for the forces and moments, oriented with the local vehicle axes and in the proper program units, had to be used to insure the rest of the subroutines would smoothly continue their regular functions. The program units for the forces were found to be pounds, and the moments were found to be in inch-pounds. By specifying the input values for the forces and locations in the units of pounds and inches, respectively, this requirement had already been met. Next, the program variable names for the x, y, and z forces and the x, y, and z moments in RESFRC were found to be SFXS, SFYS, SFZS, and SNPS, SNTS, and SNPSS, respectively.

All that remained was to set up the linear interpolation for the

forces and locations at time values between the input time values. The program variable for time was found to be T. Using the difference between T and the next smaller time step, the variable VART was created as a general percentage value from the linear interpolation method.

The mathematical operation proceeded as follows: First of all, the T which the program had progressed to had to be situated between the time step greater than T and the next smallest time step. In other words, the location of T in reference to the input time values in SUBB had to be found. That is why the sequential loadings of the time values had to be performed, because the proper orientation of the T variable used by the program could not be performed unless the time values were in sequentially increasing order. After the location of T was found using an IF statement loop, the next operation was to compute VART as a percentage value using T. This was done by dividing the difference between T and the next smallest time step by the difference between the next largest time step and the next smallest time step (both relative to T). Then, this percentage was used to compute the forces in the x, y, and z directions at the time T. Next, the x, y, and z locations at time T were found using the same linear interpolation method (and called ECKS, WHY, and ZEE, respectively).

After computing the values for SFXS, SFYS, and SFZS and the location values ECKS, WHY, and ZEE at time T, the operations were concluded by using simple equations to compute the moments SNPS, SNTS, and SNPSS. The whole operation, in computer language, was added as follows:

```
1002 I = 2
1003 IF(T.LE.SUBB(1,I)) GO TO 1004
      I = I+1
      GO TO 1003
1004 IM1 = I-1
      VART = (T-SUBB(1,IM1))/(SUBB(1,I)-SUBB(1,IM1))
      SFXS = SUBB(2,IM1)+VART*(SUBB(2,I)-SUBB(2,IM1))
      SFYS = SUBB(3,IM1)+VART*(SUBB(3,I)-SUBB(3,IM1))
      SFZS = SUBB(4,IM1)+VART*(SUBB(4,I)-SUBB(4,IM1))
      ECKS = SUBB(5,IM1)+VART*(SUBB(5,I)-SUBB(5,IM1))
      WHY = SUBB(6,IM1)+VART*(SUBB(6,I)-SUBB(6,IM1))
      ZEE = SUBB(7,IM1)+VART*(SUBB(7,I)-SUBB(7,IM1))
      SNPS = SFZS*WHY-SFYS*ZEE
      SNTS = SFXS*ZEE-SFZS*ECKS
      SNPSS = SFYS*ECKS-SFXS*WHY
```

So, the mathematical operations were confined to one subroutine, SFORCE, and were added without reducing any of the existing HVOSM capabilities. The only limitation created by this method is that the HVOSM program cannot simulate a guardrail collision and a signpost impact in the course of the same computer run. That is not considered a limitation, however, due to the rarity of the event in the normal program use.

#### Output Phase

By placing the mathematical operations in the SFORCE subroutine and using program variables for forces and moments, no additional

output statements were required for the program since the regular PRINT and OUTPUT subroutines list all the necessary output for the program results. The only additional output required by the signpost modification was the listing of the values input in the SUBB matrix.

The input variables are printed out under statements in the IDOUT subroutine. Therefore, the output modifications had to be performed on the IDOUT subroutine, once again using the COLL trigger associated with the sign impact option. The BARRIER common block had to be added to the IDOUT subroutine so that the variables would be present for output, which had been unnecessary previously (since none of the other BARRIER variables were derived directly in the input operation).

Proceeding to the end of the IDOUT subroutine, the changes were inserted immediately before the "CALL DRIVID" statement. First, the COLL trigger was added, which transferred program flow to the "CALL DRIVID" statement if COLL was not equal to 1.0. Remember, COLL was set equal to 1.0 for sign impact option operation of the HVOSM. Then, a title line which delineated the information set forth below it as "Sign Impact Force and Location Data", with a series of astericks, was set up for print. This was followed by headings for each column of matrix information: time, forces, and locations, all with the attached units. Rather than list these statements, which are merely a series of formats and variable listings, reference is made to Appendix IV, which contains the listings of all the changes mentioned in this chapter exactly as they appear in the program.

### Conclusion

While at first seeming a complicated task, the actual modification of the HVOSM was performed quite easily following proper program analysis. All of the changes were made without reducing the HVOSM capabilities existing before the modifications. All of the changes were made in the simplest manner possible, and each of the changes was accompanied by commentary blocks to identify the changes and their purpose. Appendix IV contains the actual program listings of the changes and the comments which precede them.

### CHAPTER III PROGRAM VALIDATION

#### General Approach

With the completion of the HVOSM program modification, the only task required before the actual sign impact parameter study was the validation of the modified program. Even though the HVOSM was a proven program before the changes were made, the modified HVOSM had to demonstrate operations which could duplicate real conditions as closely as possible. To that end, a series of tests were arranged to prove that the program could match theoretical results, and also that it could approximate the results of actual crash tests using limited crash test data.

The series of four validation exercises were arranged in order of increasing complexity. First of all, a simple linear deceleration example was performed to compare theoretical results with program results. Secondly, a LaGrangian analysis of a sample vehicle with a constant force aligned with the vehicle axis was used in a comparison between theoretical and program simulated planar motion. After the successful completion of these two tests, the next two exercises were trials at duplicating actual crash test results. The crash tests in question were crash tests #11 and #9, performed as described in reference 7. While the only data used in duplication of those tests were the accelerometer readouts (along with all the vehicle parameters), the program still closely approximated the actual results of the tests. A closer examination of each of the exercises will reveal the function

of each in confirming the validity of the modified HVOSM.

The test vehicle parameters for the theoretical tests were taken from the HVOSM User's Manual (3). These parameters were taken for a standard sized car, and the tests were run using a frictionless road both for the theoretical analysis and the program simulation. The crash tests provided particular vehicle parameters for the automobile used in the crash tests, so the input data reflected a particular automobile make and model (1971 Vega) and a proper surface with a friction factor of .5.

#### Linear Deceleration

The linear deceleration test was a basic test of the proper functioning of the modified HVOSM. The program was run after theoretical analysis showed a required force of 6829.02 pounds applied for 1.5 seconds to the center of gravity to stop the sample vehicle with a forward speed of 60 miles per hour. The theoretical equation used for this simple test was:

$$M\Delta V = F\Delta t$$

Concentrating the impulse force at the sprung mass center of gravity to duplicate the lumped mass assumption of the theoretical analysis, the HVOSM results were hopefully to agree very closely with the theoretical results. The actual comparison of the results, shown as a graph of the automobile velocity versus time for both the theoretical results and the HVOSM program output, appear in Figure 1 as a simple line.

Figure 1 confirms the basic soundness of the modified HVOSM. The results agree almost exactly, with the greatest variation between

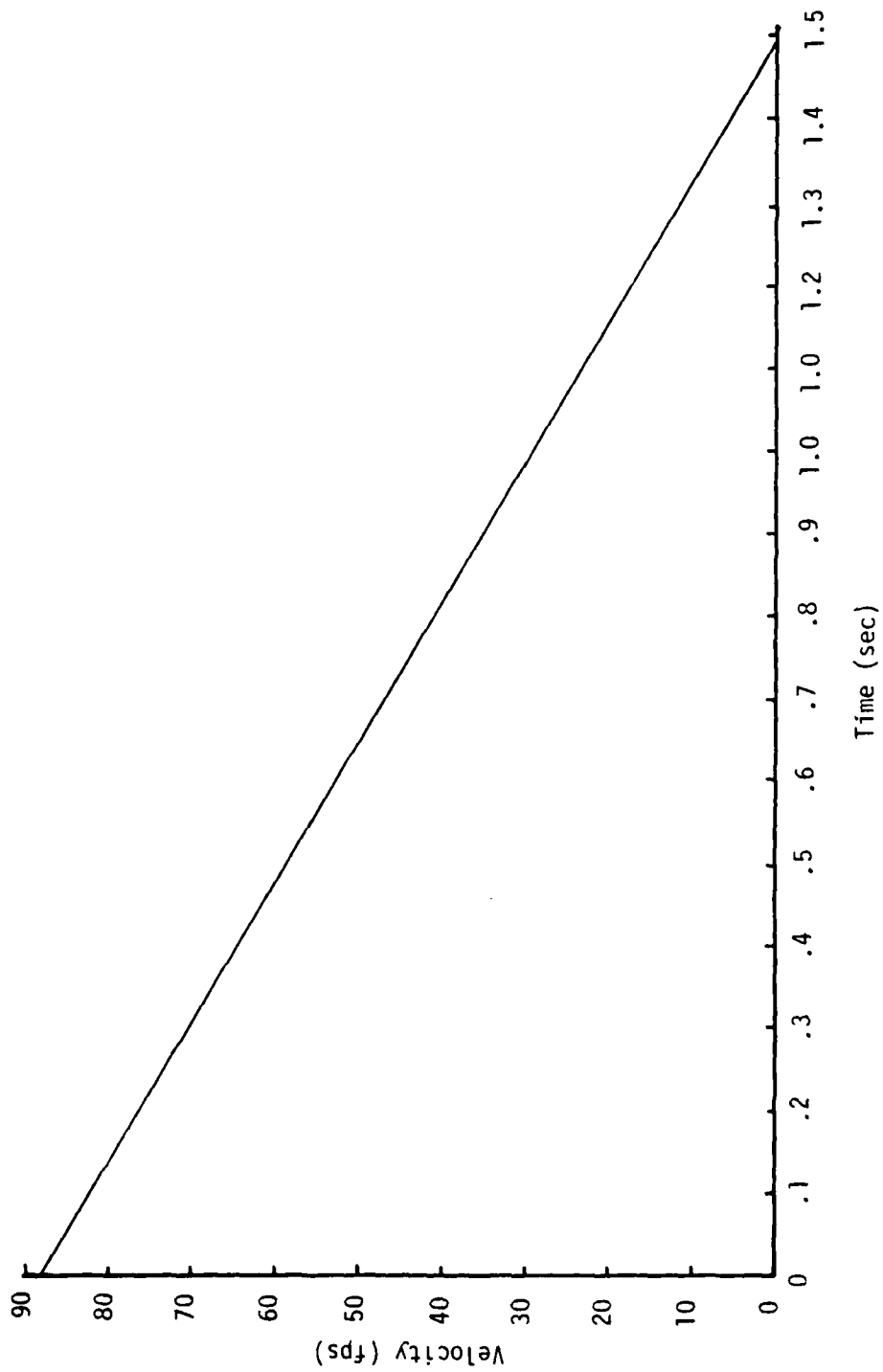


Figure 1. Linear Deceleration Test.



program results and the theoretical results only a negligible .02 feet per second. This is why the results of both are represented by a single line -- the differences were too small to appear on the graph. The very fact that the theoretical lumped mass comparison agreed so closely with the HVOSM's complex automobile model is an affirmation that the program is basically sound. The subsequent tests will determine if the more complex problems can be handled by the modified HVOSM in like manner.

#### LaGrangian Analysis

With the basic program functioning assured, the next test was to prove the program could operate in two dimensions and approximate theoretical results. The theoretical problem for this test was chosen as a simple application of a constant force to a moving automobile. The constant 200 pound force was to be applied to the front of the automobile in the negative vehicle x-axis direction, that is, aligned constantly towards the rear of the vehicle. A LaGrangian analysis of the system was then performed using the test problem. The global and local coordinate systems used in the analysis are shown in Figure 2.

LaGrange's equation, simply stated, is

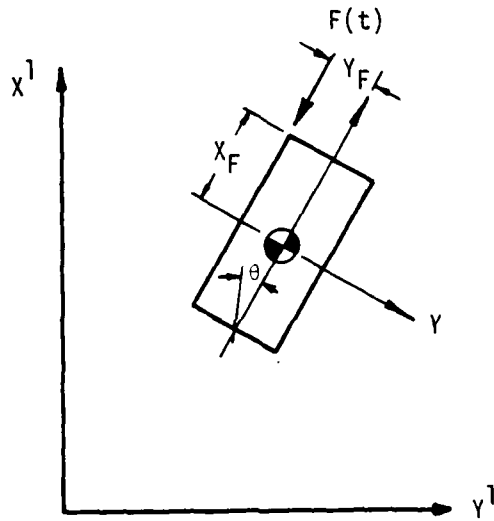
$$\frac{d}{dt} \left( \frac{\partial U}{\partial \dot{q}_i} \right) - \frac{\partial U}{\partial q_i} + \frac{\partial V}{\partial q_i} = \frac{\partial Q_e}{\partial q_i} \quad (1)$$

where

U = kinetic energy

V = potential energy

Q<sub>e</sub> = work done by applied external forces



Global Coordinates:  $x^1, y^1, \theta$   
Vehicle Local Coordinates:  $(X, Y)$

Figure 2. LaGrangian Coordinate Systems.

$q_i$  = a generalized (global) coordinate

$\dot{q}_i$  = the first time derivative of the generalized coordinate

Expressing the equation variables in terms of global coordinates,

$$U = \frac{1}{2} m v^2 + \frac{1}{2} I \dot{\theta}^2 \quad (2)$$

$$v^2 = \dot{x}'^2 + \dot{y}'^2 \quad (3)$$

There are no potential energy terms for this problem, so that term can be excluded from the equation. That leaves the external work term to be defined in terms of the generalized coordinates:

$$Q_e = F_x x'_F + F_y y'_F \quad (4)$$

where

$$x'_F = x' + x_F \cos\theta + y_F \sin\theta \quad (5)$$

$$y'_F = y' + x_F \sin\theta - y_F \cos\theta \quad (6)$$

and

$$F_x = F(t) \cos\theta \quad (7)$$

$$F_y = F(t) \sin\theta \quad (8)$$

Now that all the terms are defined, each of the three equations can be extracted by allowing  $q_i$  to be equal to  $x'$ ,  $y'$ , and  $\theta$  in LaGrange's equation -- that is, equation 1.

$$U = \frac{1}{2} m(\dot{x}'^2 + \dot{y}'^2) + \frac{1}{2} I \dot{\theta}^2 \quad (9)$$

$$\frac{\partial U}{\partial x'} = 0 \quad (10)$$

$$\frac{\partial U}{\partial y'} = 0 \quad (11)$$

$$\frac{\partial U}{\partial \theta} = 0 \quad (12)$$

$$\frac{d}{dt}\left(\frac{\partial U}{\partial \dot{x}'}\right) = \frac{d}{dt}(m\dot{x}') = m\ddot{x}' \quad (13)$$

$$\frac{d}{dt}\left(\frac{\partial U}{\partial \dot{y}'}\right) = \frac{d}{dt}(m\dot{y}') = m\ddot{y}' \quad (14)$$

$$\frac{d}{dt}\left(\frac{\partial U}{\partial \dot{\theta}}\right) = \frac{d}{dt}(I\dot{\theta}) = I\ddot{\theta} \quad (15)$$

Combining equations 4, 5, and 6 for the expression for  $Q_e$ ,

$$\frac{\partial Q_e}{\partial x'} = F_x = F(t) \cos\theta \quad (16)$$

$$\frac{\partial Q_e}{\partial y'} = F_y = F(t) \sin\theta \quad (17)$$

$$\frac{\partial Q_e}{\partial \theta} = F_x(-x_F \sin\theta + y_F \cos\theta) + F_y(x_F \cos\theta + y_F \sin\theta) \quad (18)$$

Therefore, the three equations for theoretical analysis end up as

$$m\ddot{x}' = F(t) \cos\theta \quad (19)$$

$$m\ddot{y}' = F(t) \sin\theta \quad (20)$$

$$I\ddot{\theta} = 2F(t)y_F \quad (21)$$

Since  $F(t)$  is constant, the  $\ddot{\theta}$  acceleration is constant and the  $\ddot{x}'$  and  $\ddot{y}'$  accelerations are only dependent on  $\theta$ . The rest of the theoretical analysis, which consisted of vehicle location, velocity, and yaw speed calculations at .02 second time intervals, was performed using simple equations of motion:

$$\dot{x} = \dot{x}_{OLD} + \ddot{x}\Delta t \quad (22)$$

$$x = x_{OLD} + \dot{x}_{OLD}\Delta t + \frac{1}{2} \ddot{x}\Delta t^2 \quad (23)$$

These equations were applied to each of the three variables in the correct order, since the accelerations in the  $x'$  and  $y'$  directions were dependent on the value of  $\theta$  from the previous time step.

After the LaGrangian analysis for the constant 200 pound force was completed using the same vehicle parameters that were used for the HVOSM program input, the results of each form of analysis were graphically compared in Figures 3 through 6. Each of the graphs differ only after a significant period of time, and even then the differences are very small. Figure 3, the comparison of velocities in the local vehicle x-direction, shows the results differing by 1.57 feet per second at the end of 1.5 seconds, an error of only 3.8%. The graph of the velocities in the vehicle y-direction, shown in Figure 4, reveals a maximum difference of 1.31 feet per second between the two methods of analysis, an error of 2%. In Figure 5, which is the graph of the vehicle location along the global x-axis, the results agreed so closely that only one line could be presented. The maximum difference was only 1.33 inches in 214.8 feet, representing virtually exact agreement. Finally, Figure 6, the vehicle yaw speed, shows a maximum difference of 1.18 degrees per second, an error of only 2.6%.

These results served to complete the validation of the modified HVOSM in reference to theoretical analysis. Using linear deceleration and LaGrangian analysis, the program was examined for soundness in both linear and planar motion. The LaGrangian analysis, involving two dimensions, provided a number of variables which were used to evaluate the HVOSM program results. Each comparison served to further support the validity of the modified HVOSM, revealing only negligible error attributed mainly to the lumped mass approximations used for the inertial properties in the theoretical analysis.

Since the HVOSM was developed from theory, reliable duplication of

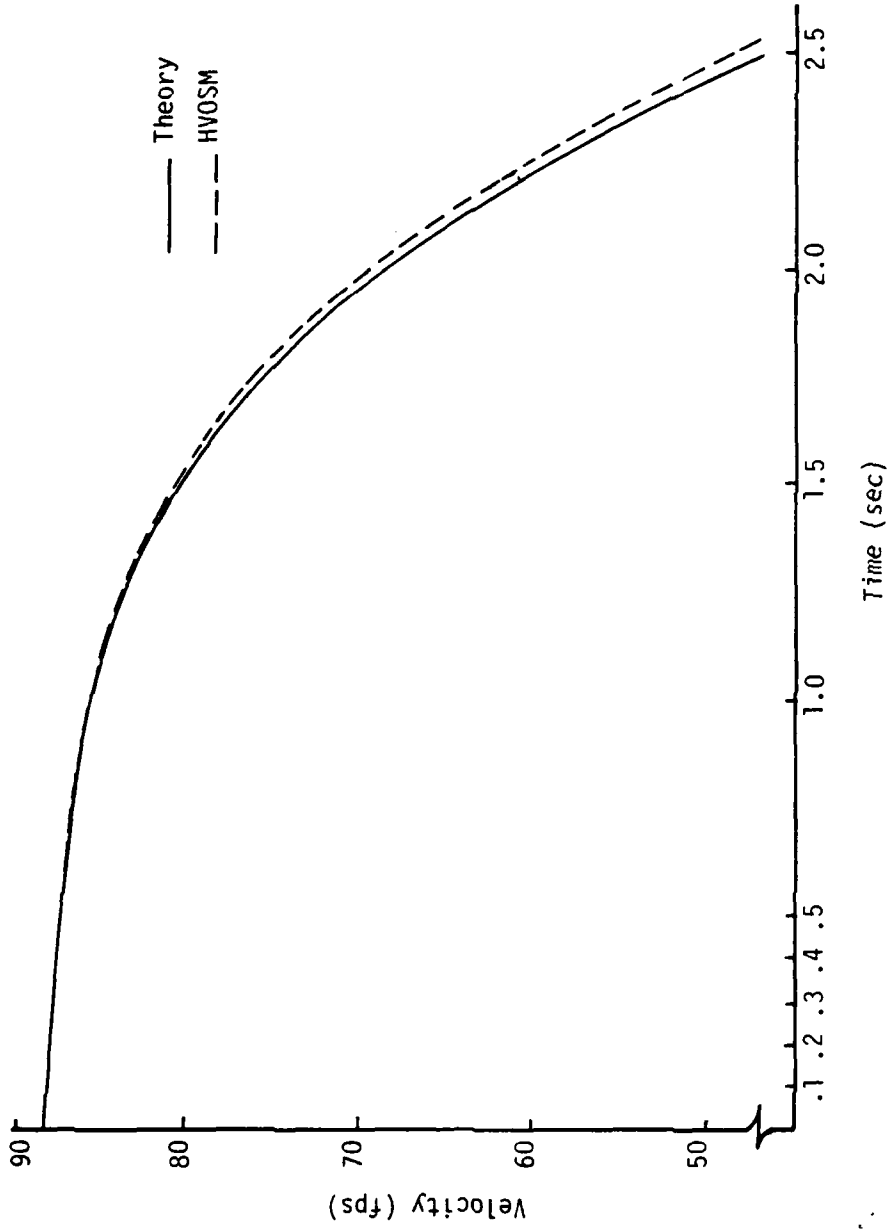


Figure 3. Velocity of Vehicle in Local X Direction.

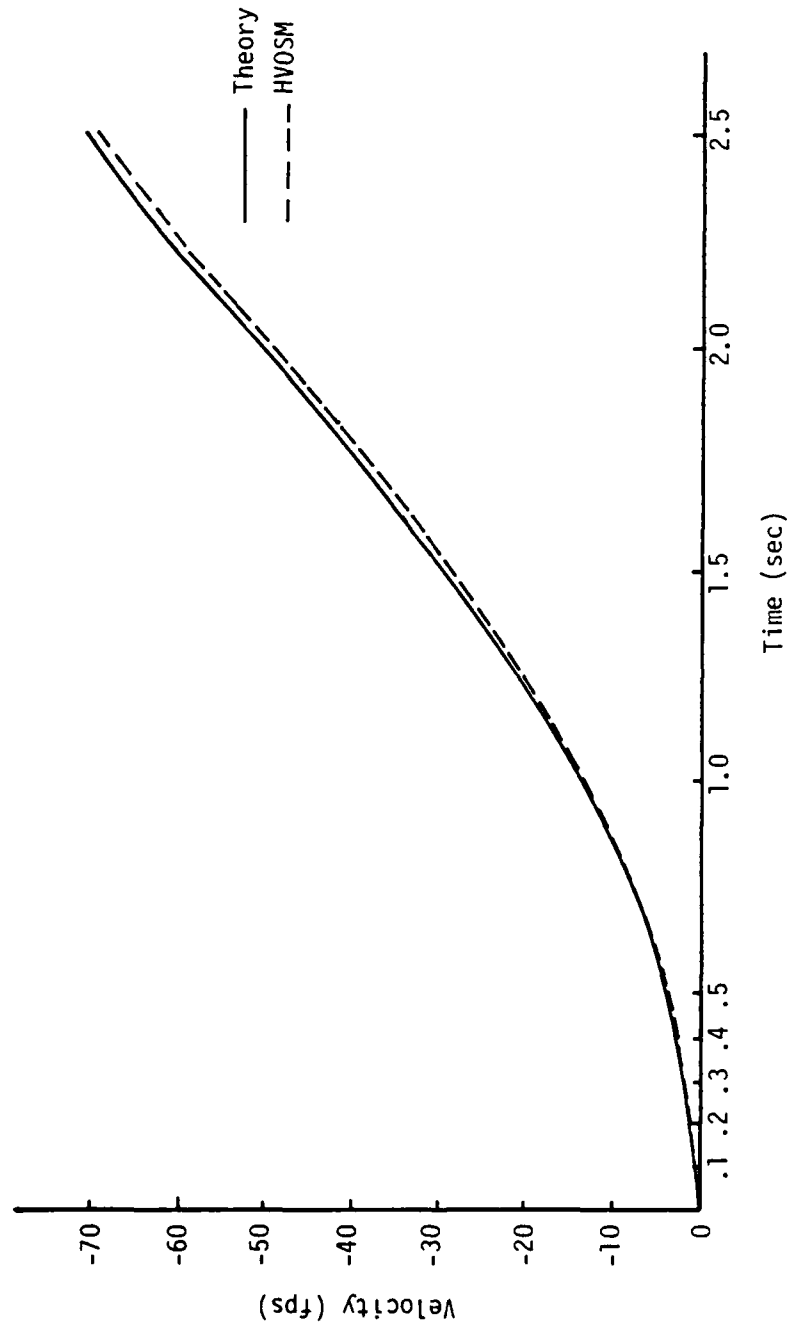


Figure 4. Velocity of Vehicle in Local Y Direction.

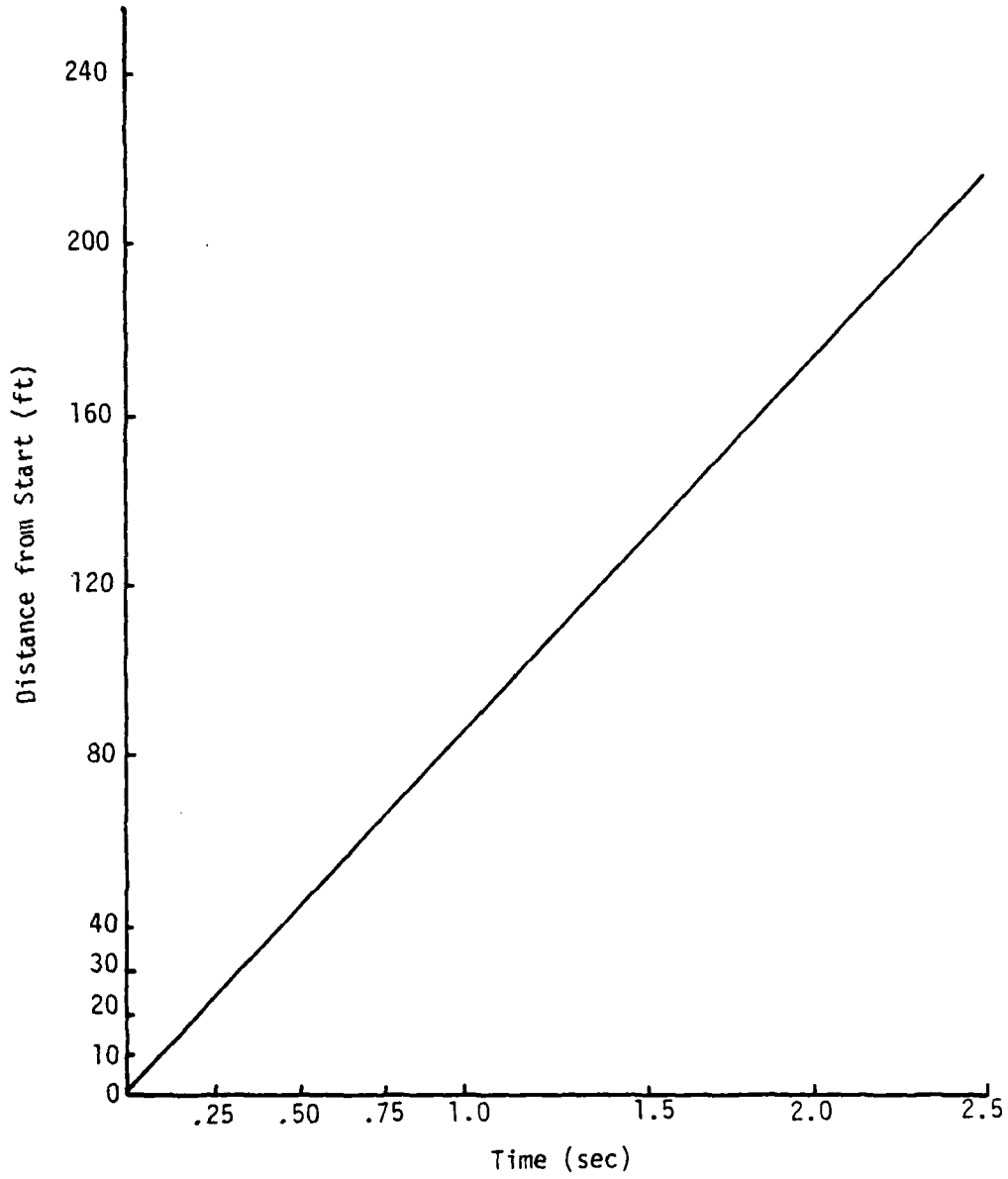


Figure 5. Vehicle Location Along Global X Axis.



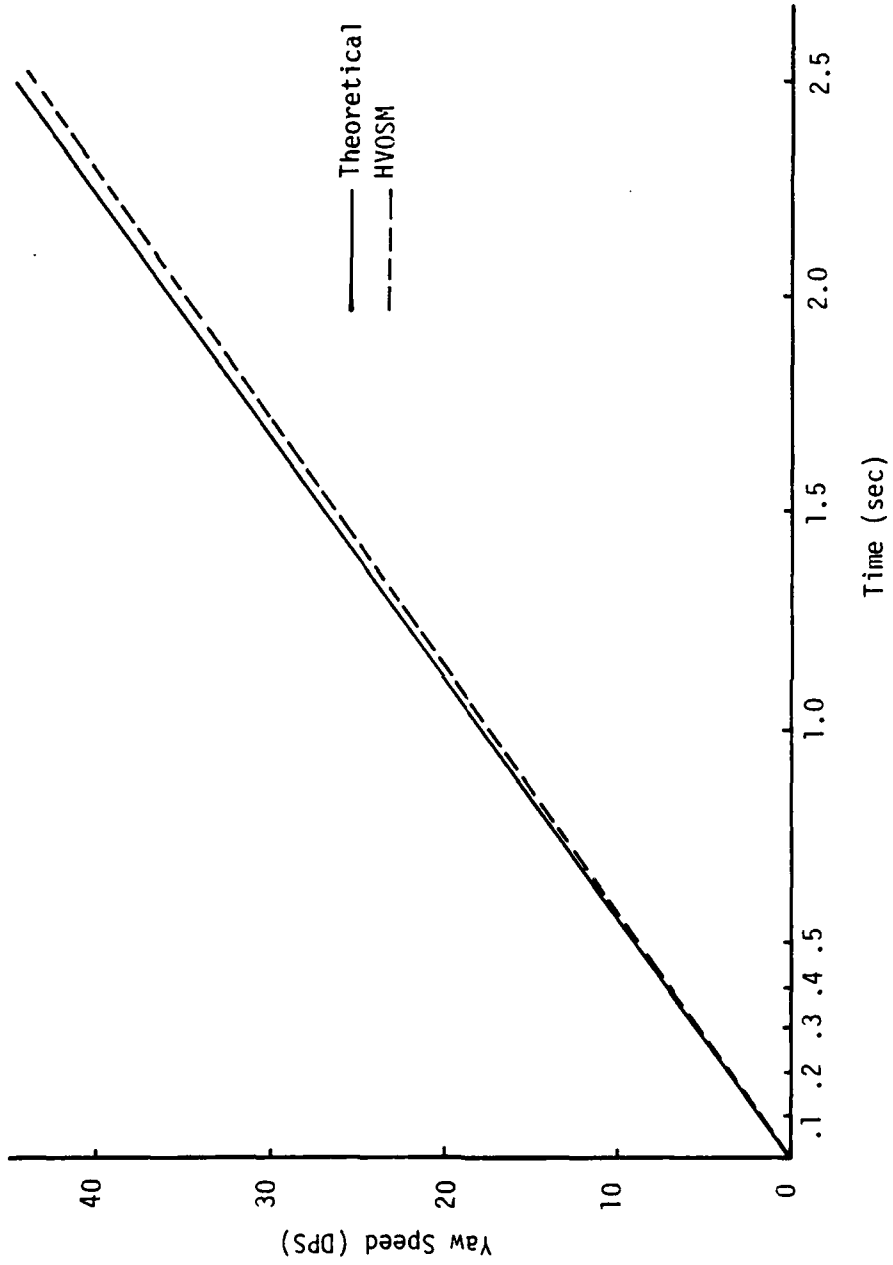


Figure 6. Vehicle Yaw Speed.

theoretical results was expected. The sprung mass, with its six degrees of freedom, and the vertical deflections of the four unsprung mass (wheels) provide only ten degrees of freedom, with a possible eleventh degree of freedom using the free steering mode of program operation (as all these tests did). The next, more difficult hurdle was the duplication of results of actual crash tests, with their three-dimensional motion and infinite degrees of freedom.

#### Crash Test Number 11

Duplication of real-world signpost collisions is the central function of the modified HVOSM. Necessarily, the program had to prove itself by duplicating the results of previous crash tests before it could be used with confidence. The first crash test chosen for this final phase of validation was crash test #11 (7) as performed by TTI. Accelerometers had been placed on the vehicle and those readouts were available, along with the change in momentum at .183 seconds after the collision and the approximate time that vehicle rollover started (this vehicle rolled over in the test). The fact that the vehicle actually rolled over was an important factor which the HVOSM had to be able to duplicate.

The test vehicle, a Vega, was well documented so that the input parameters were assured to match the test vehicle (2). Figure 7 lists the card images of the input for the modified HVOSM simulation. The variables associated with the input numbers in Figure 7 can be found in the HVOSM User's Manual (3). The accelerometer readings from the right side of the vehicle were used as direct approximations of the horizontal

INPUT HEAD BY CALSWA										
	.25	.005	1.0	.005	70.	0.0	0.0	-1.0	25	
1.0	424	.575	386.4	1672.4	100.34	13045.	1.0	250.		1
4.876	5213	55.1	34.1	9.5	1.31	0.0	-100.	3625.		2
42.57	5			.001	0.0	0.0	11.83			3
16.										4
1215.	6	10.	7.11	234.	11690.	.5	.85	-6.01		5
1240.		0.0	0.0	0.0	0.0	0.0	0.0	5500.		6
0.0		-19.92	1880.6	0.0	0.0	0.0	0.0			7
-36.	4.	1.	-36.	-9.	8.					8
-4.										9
										10
										11
										12
										13
										14
										15
										16
										17
										18
										19
										20
										21
										22
										23
										24
										25
										26
										27
										28
										29
										30
										31
										32
										33
										34
										35
										36
										37
										38
										39
										40
										41
										42
										43
										44
										45
										46
										47
										48
										49
										50
										51
										52
										53
										54
										55
										56
										57
										58
										59
										60
										61
										62
										63
										64
										65
										66
										67
										68
										69
										70
										71
										72
										73
										74
										75
										76
										77
										78
										79
										80
										81
										82
										83
										84
										85
										86
										87
										88
										89
										90
										91
										92
										93
										94
										95
										96
										97
										98
										99
										100

Figure 7. Input for Crash Test Comparisons.

forces generated in the collision. This was because the signpost impacted 15 inches to the right of center, so that accelerometer was closest to the lateral point of contact. Then, since the post had bent around the hood of the car and imparted large vertical forces to the front of the car, the vertical forces were successively approximated until the HVOSM results matched the crash test results. The final applied vertical impulse appears in Figure 8. The point of application for the horizontal and vertical impulses was 15 inches to the right of center on the front bumper, just as in the crash test. Also, the accelerometer placements on the simulated HVOSM vehicle matched those on the actual crash test vehicle.

The results of the simulation are shown in Table 1 and Figure 9. Using all of the available recorded data to check the accuracy of the modified HVOSM program simulation, the program results matched extremely well with the crash test #11 results. As shown in Table 1, the maximum error was below 10% (except for isolated accelerometer points), and the accelerometer readings, both taken from the right accelerometer of the vehicle shown in Figure 9, correlate very closely. The simulated vehicle rolled, as did the test vehicle, and at almost the same time. Based on relatively little data, the modified HVOSM was able to duplicate almost exactly the results of crash test #11. Just to prove that this was not an isolated success, a second crash test exercise was chosen as a final challenge to the acceptance of the modified HVOSM.

#### Crash Test Number 9

Crash test #9 (7), as performed by TTI, was similar to crash test #11 in many ways. Crash test #9 used the same Vega, used the same

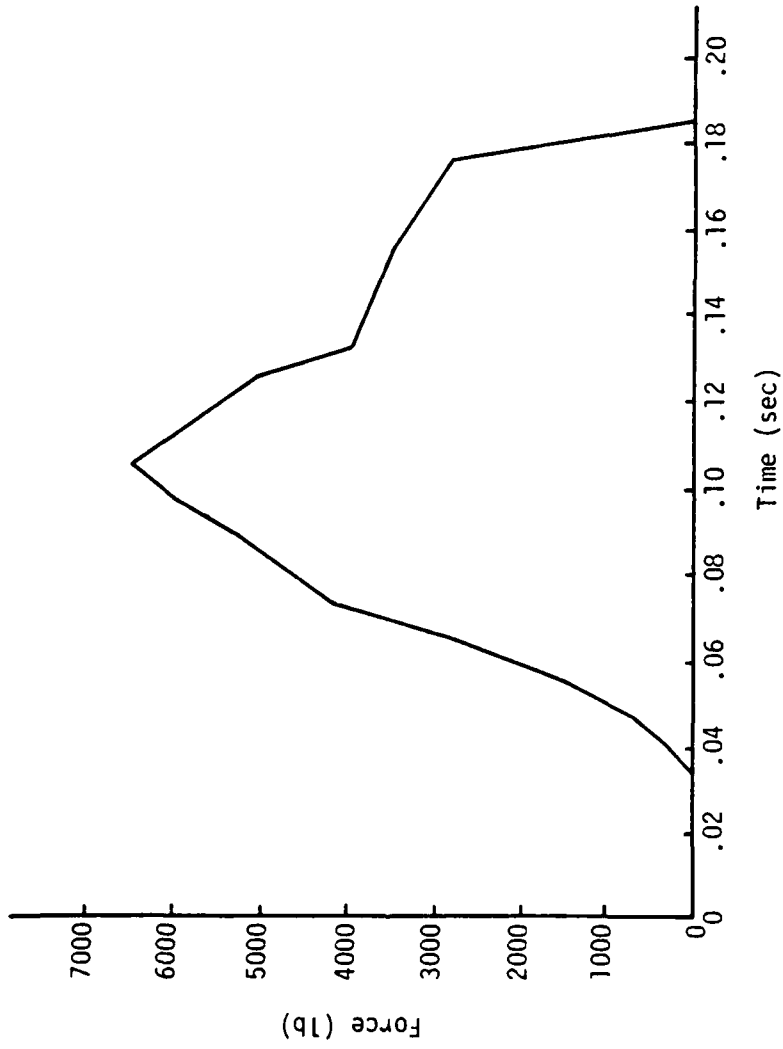


Figure 8. Vertical Impulse Input for Crash Test #11 Duplication.

TABLE 1. Crash Test #11 Duplication.

	TEST	HVOSM	ERROR
Change in Momentum (lb-s)	1433	1536	7.2%
Start of Roll (sec)	.24	.24	---
Peak Deceleration (G's)	7.67	7.42	3.3%

TABLE 2. Crash Test #9 Duplication.

	TEST	HVOSM	ERROR
Change in Momentum (lb-s)	2363	2419	2.4%
Back Wheels Leave Ground (sec)	.183	.19	---
Peak Deceleration (G's)	13.	12.89	.85%

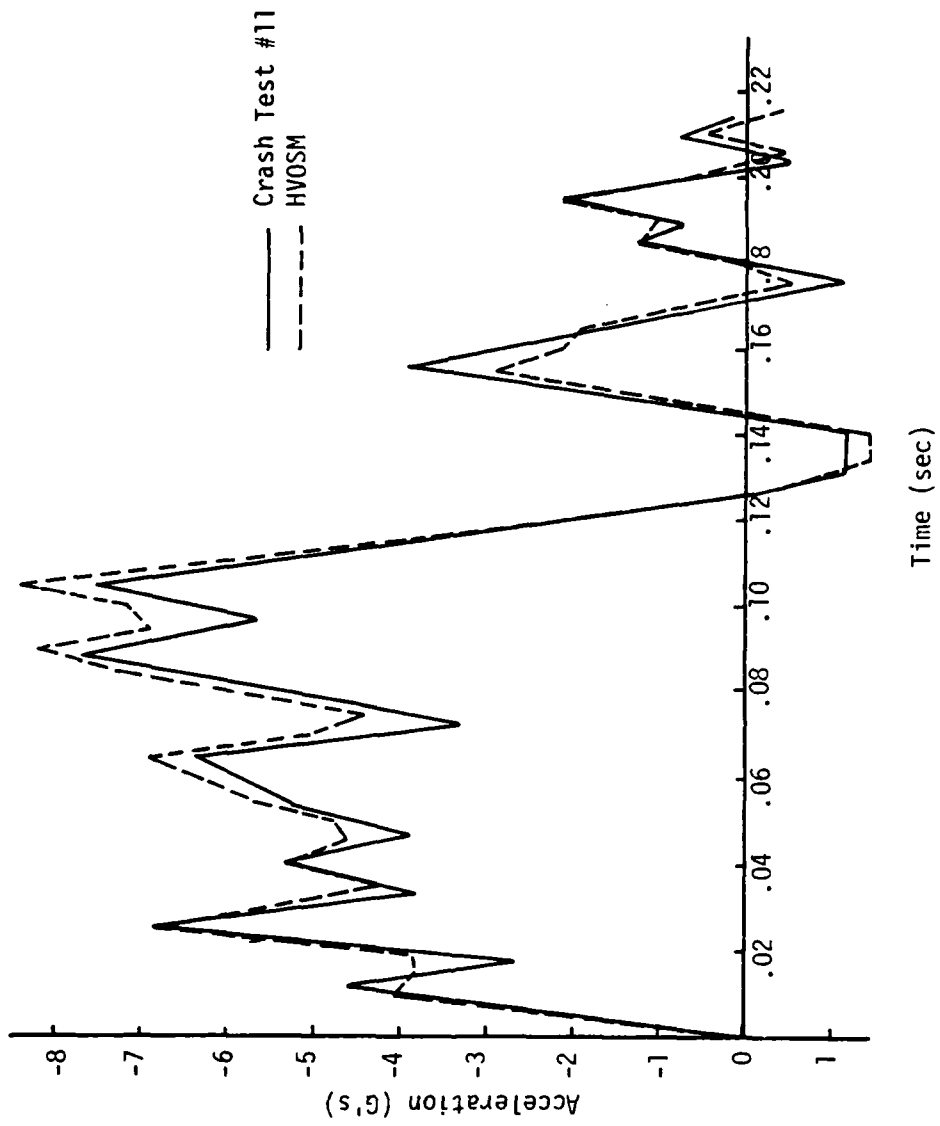


Figure 9. Right Accelerometer Readouts.

accelerometer placement, and had the same type of recorded data as crash test #11. There were some challenging differences, however. First of all, the impact occurred 15 inches to the left of center, so the left accelerometer readouts were used to simulate the horizontal impulse forces with time. Second of all, the signpost was markedly different and much stiffer than AASHTO standards. While the signpost in crash test #11 was not AASHTO-approved, the signpost in crash test #9 was far in excess of AASHTO standards, and as such represented an extreme test. Finally, the automobile nearly rolled, but it did not experience rollover even though the signpost wrapped around the vehicle front as in crash test #11. Therefore, the challenge was to take the car to the brink of rollover but not over it, while duplicating the rest of the test results as closely as possible. Using successive approximations, as in the crash test #11 duplication, the final vertical sign impulse input developed for the exercise is shown in Figure 10.

As seen in Table 2 and Figure 11, the modified HVOSM came even closer to matching the actual crash test results than in the previous exercise. The errors were more than halved from what they were in the crash test #11 effort, and the accelerometer readouts in Figure 11 once again shadowed those of the actual crash test. The vehicle lost ground contact on three of the four wheels, but did not roll over, just as had been planned. Another result, not shown in the table or on a graph, was that it took only one-third of the number of iterations used in the exercise for crash test #11 to duplicate crash test #9. In other words, experience made the validation exercise easier to complete.



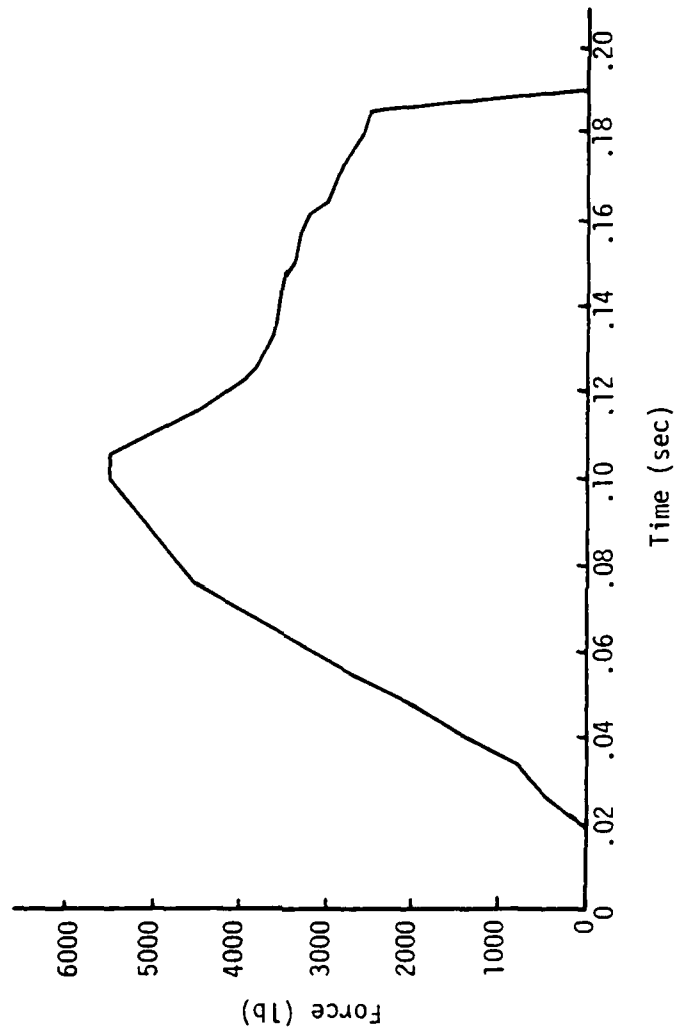


Figure 10. Vertical Impulse Input for Crash Test #9 Duplication.

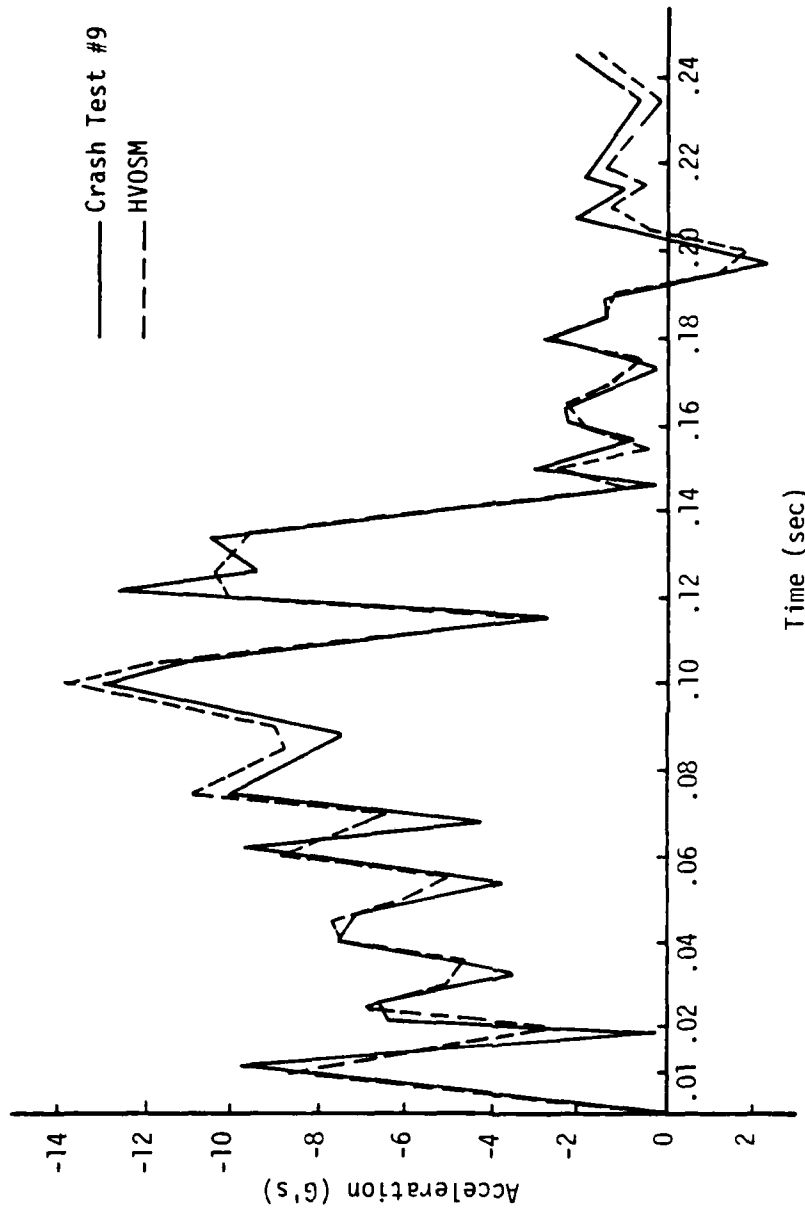


Figure 11. Left Accelerometer Readouts.

Another interesting sidelight can be observed by comparing the signpost vertical impulses for the two crash tests, shown in Figure 8 (p. 32) and Figure 10 (p. 36). Two different signs, both of which did not break away but which bent around the hood and caused large vertical impulses, almost matched vertical impulse curves in separate development of each curve. The vertical impulse of the crash test #11 curve was 547 pound-seconds, while the vertical impulse of the crash test #9 curve was 561 pound-seconds, a spread of only 1.3%. This coincidence was used later to define the vertical impulse in the parameter study.

#### Conclusion

The modified HVOSM had to prove its validity by comparison with both theory and actual signpost impact test results. Completing each challenge, the modified HVOSM was shown to be reliable and easy to use. The error in many cases was negligible, and the duplications were accurate for even the most complex tests. Using relatively sparse amounts of crash test data, the modified HVOSM was able to duplicate two different signpost collisions almost exactly, matching all measured output from the real crash tests. With the completion of this phase of the thesis, the parameter study of signpost impacts could be realistically and authoritatively examined.

## CHAPTER IV PARAMETER STUDY APPLICATION

### Introduction

After proving the modified HVOSM to be an accurate simulator of signpost collisions, the crux of the thesis could be properly approached. AASHTO standards, as mentioned at the start, were developed before the trend toward subcompact cars became evident. Since no parameter studies comparing the effects of different sized cars in collisions with a signpost meeting the upper limit of AASHTO standards had been performed, the HVOSM was modified for the purpose of just such a parameter study.

Using the same horizontal and vertical impulses on each size car, all approaching at the same speed before the collision, the modified HVOSM was used to compare the effects of these impulses on the different automobiles. Two different signpost types were used: the break-away model, which consisted of only horizontal impulses; and the base-bending model, which consisted of both horizontal and vertical impulses. The automobile parameters were input for a large car, a medium car, a compact car, and a subcompact car. The credibility of the parameter study can be better shown by examining the preparation of the sign and automobile models upon which the study results were based.

### Signpost Models

As mentioned above, two signpost models were used in the study. The models were developed using AASHTO standards (10) and the results

of the validation tests. The AASHTO standards, in brief, limit the change in momentum to 1100 pound-seconds for a 2250 pound automobile striking a support at speeds between 20 and 60 miles per hour. These specifications apply for both breakaway signposts, which are designed to break away at ground level, and base-bending signposts, which bend at the base as the vehicle rides down the length of the signpost. These two signpost models required impulses to fit the AASHTO specifications.

The breakaway model signpost was composed of only horizontal impulses. The horizontal impulse, shown in Figure 12, was developed using the left accelerometer readout from crash test #11 (7), and the total impulse is 1095 pound-seconds, just less than the upper limit set by AASHTO. Examining Figure 12 in detail, the total impulse up to .185 seconds is 1095 pound-seconds, with the subsequent impulses negating each other arithmetically. That .185 second impulse value is important because it is the time point used to calculate the change in momentum in each program simulation. This signpost impulse was used for the breakaway model impact simulation input with each vehicle size, from large to subcompact.

The base-bending model signpost was composed of both horizontal and vertical impulses. The horizontal impulse used was the same as that used in the breakaway model. This choice was made assuming that the same signpost used in the breakaway model was driven into the ground rather than mounted to break away at the base. The vertical impulse, produced as the signpost wrapped around the front of the vehicle, was taken as a combination of the vertical impulses found in

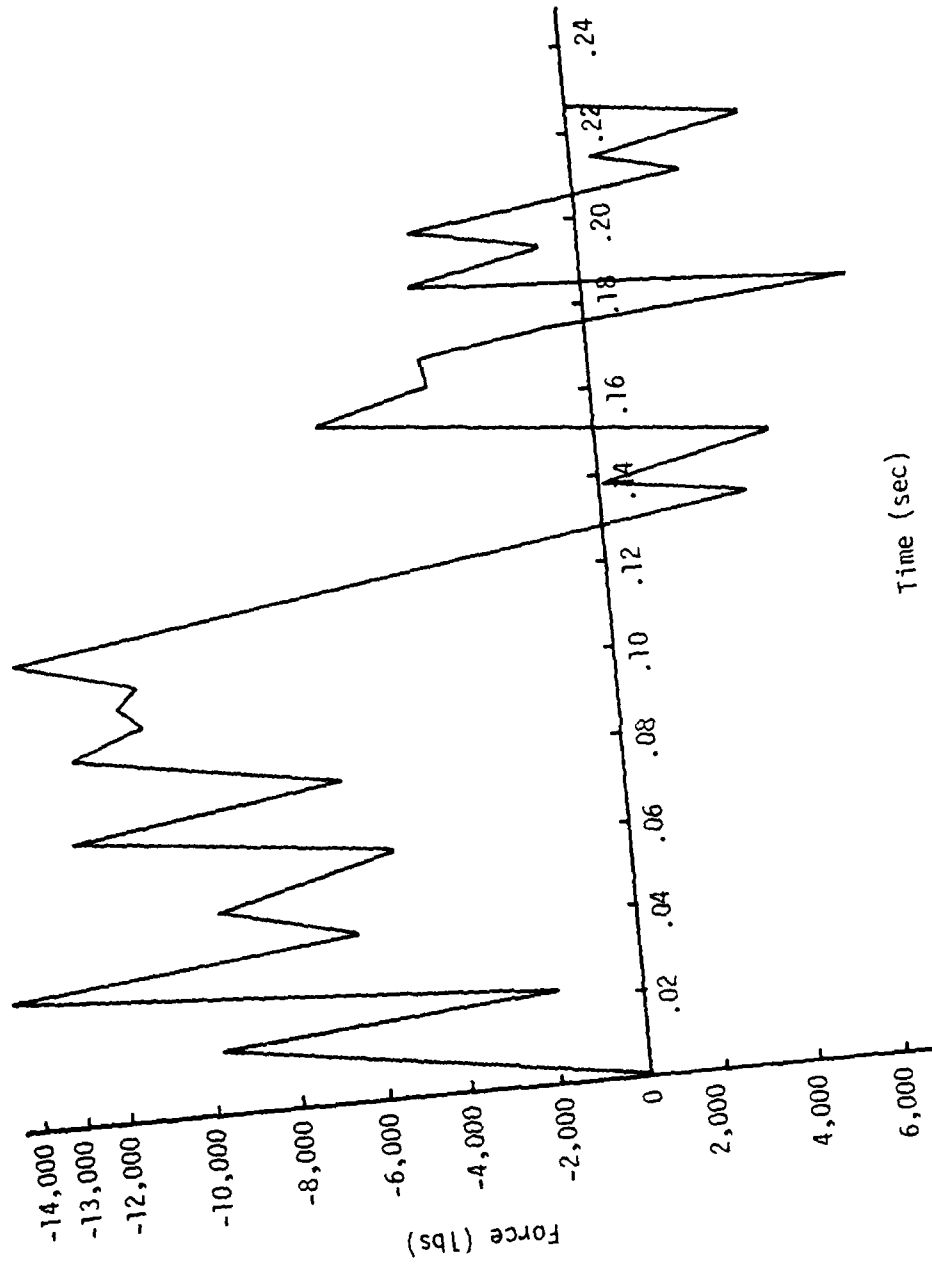


Figure 12. Horizontal Impulse Input for All Cars.

the duplication of crash tests #11 and #9. As previously noted, the impulses of those crash tests were 547 pound-seconds and 561 pound-seconds for tests #11 and #9, respectively. Since these two different posts applied almost identical vertical impulses in base-bending signpost impacts, the vertical impulse for the base-bending model was based on these impulses. The resultant vertical impulse, shown in Figure 13, measured 567 pound-seconds. The small error is due to the fact that the time points had to be those used for the horizontal impulse input, since the horizontal impulse was most critical. The input, after adjusting to the horizontal impulse time steps, contained some roundoff errors in the vertical impulse which accounted for the small impulse increase.

In short, the breakaway model and the base-bending model were based on AASHTO standards and actual crash test results. The breakaway model consisted of a horizontal impulse only, while the base-bending model consisted of both horizontal and vertical impulses to simulate the effects of a signpost wrapping around the front of the vehicle as the car rides down the signpost. Both models were developed for impact by the four car sizes to examine how the same signposts could affect different sizes of automobiles in a collision. With the completion of the signpost models, the only required input development was the car data for the operation of the HVOSM simulations.

#### Vehicle Data

Four vehicle sizes were used in this parameter study: large, medium, compact, and subcompact. Each of these had to be defined as

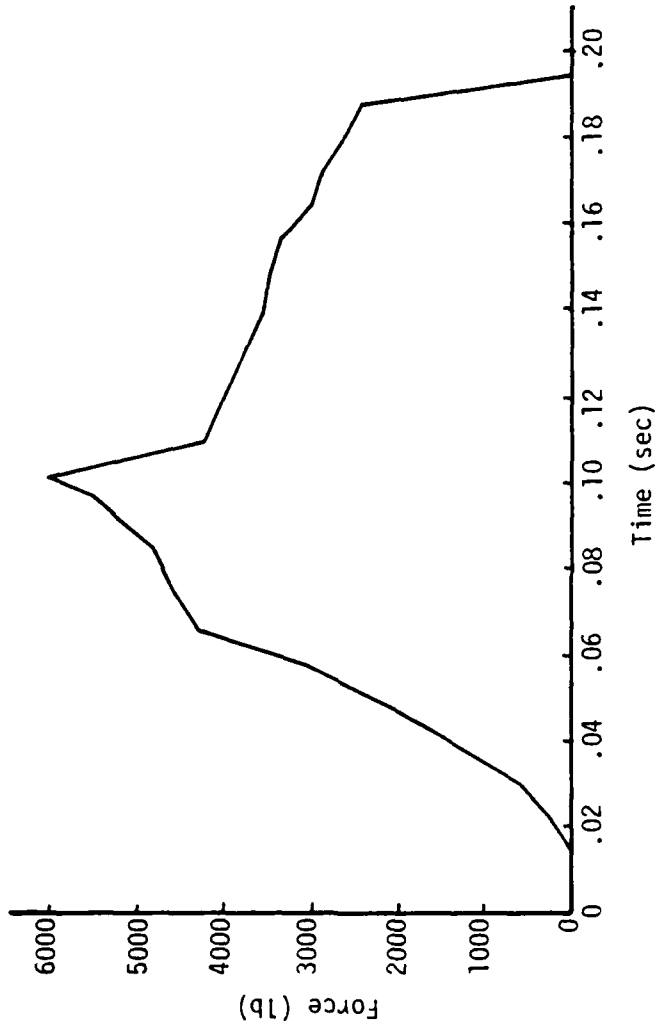


Figure 13. Vertical Impulse Input for All Cars.



accurately as possible for the program input variables. In some cases, the car data were incomplete, so that other data which would least affect the results were substituted. For example, the medium and sub-compact cars lacked some minor program values, so the values for the large and compact cars, respectively, were used for those gaps in the data. It was felt that using the data from the next largest vehicle than the one lacking data would at least serve to prevent exaggeration of program results. To illustrate, using large car suspension data for the medium car would moderate the results to a degree, while using the compact vehicle's suspension data might magnify the impact effects on the medium car. Also, each vehicle had the impulse positioned on the front bumper 15 inches to the right of center. Since the front bumper is approximately at the same height as the center of gravity, no displacement along the vehicle z-axis was input for any car, but the distance to the front bumper measured along the vehicle x-axis from the center of gravity varied with the car size.

Several other parameters, none associated with a particular car, were input in all cases. The road surface coefficient of friction was set at .5 for all tests, even though many tire manufacturers claim a friction factor of .8. This decision was made based on the fact that signposts are placed off the road shoulder and not on a paved surface. All vehicles approached impact at 60 miles per hour, corresponding to the upper limit set in the AASHTO standards. All tests were performed using the free-steering mode of the modified HVOSM operation to study the free-wheel stability of the vehicle in post-impact motion. Finally, all program simulations were run for 3 seconds, which was a long enough

time to observe the important accelerations and vehicle motions.

Large car. One of the two well-documented vehicles, the large car was represented by a 1963 Ford sedan (2). All vehicle data necessary for the modified HVOSM were available, and the input as loaded for the program appears in Figure 14. The data set ICARD values appear as the last number in every line. As can be seen by examining the ICARD=29 series, the collision input data is for the breakaway model signpost as distinguished by the lack of z-forces in the data. As explained in the crash test duplication efforts, the variables associated with each number can be found using the HVOSM User's Manual (3). An explanation of each variable as presented in the input would be tedious and detract from the main points of the parameter study.

Medium car. While the large car input was handled easily, the data for the medium car posed some problems. No complete listing of the required variables was available for the medium car. After a search, the best source was found in a compilation of vehicle data for parameter studies (1). This listed many of the required variable values for a general medium car, composed of the average values for many medium cars and thus not associated with a make or model year. While incomplete, the data were the best which could be found, and all gaps were filled using the large car data. The important and most influential variables for the study, however, were supplied in the medium car data; and the large car data were required mainly to fill out the required input. As shown in Figure 15, the medium car input was therefore more nearly correct than the inclusion of large car data might make it seem. To emphasize, the large car data were used for

INPUT READ BY CALSVA									
1.0	3.	.002	1.0	.02	70.	0.0	0.0	0.0	1
4.32	608	745	366.4	6000.	14600.	35000.	1.0	-1.0	30
52.8	56.45	61.2	80.5	5.421	11.292	22.0	-197.	475.6	3
131.	5	1.75	1.75	37.	.001	20600.	14.	4400.	4
1098.	8.	10.	6.70	200.	1.071	5284.	46.52	408	5
0.0	0.0	-22.4	104.6	0.0	0.0	0.0	0.0	1900.	6
0.0	5.	1.	0.0	15.	-8.				9
									12
PHIC(1)=1. 11									
	-5.700	-1.000	-2.450	-1.300	-0.400	0.300	0.300	-0.400	-1.300
300.	0	1000.	0	100000.001	1.5	0.0	0.0	0.0	14
0.0	0.0	0.0	0.0	0.0	15.	0.0	0.0	0.0	17
0.15	-9731.	0.0	0.0	0.0	15.	0.0	0.0	0.0	29
0.02	-1930.	0.0	0.0	0.0	15.	0.0	0.0	0.0	29
0.03	-14486.	0.0	0.0	0.0	15.	0.0	0.0	0.0	29
0.037	-8376.	0.0	0.0	0.0	15.	0.0	0.0	0.0	29
0.056	-5324.	0.0	0.0	0.0	15.	0.0	0.0	0.0	29
0.066	-12831.	0.0	0.0	0.0	15.	0.0	0.0	0.0	29
0.075	-6425.	0.0	0.0	0.0	15.	0.0	0.0	0.0	29
0.085	-12597.	0.0	0.0	0.0	15.	0.0	0.0	0.0	29
0.091	-10931.	0.0	0.0	0.0	15.	0.0	0.0	0.0	29
0.097	-11823.	0.0	0.0	0.0	15.	0.0	0.0	0.0	29
0.101	-11015.	0.0	0.0	0.0	15.	0.0	0.0	0.0	29
0.109	13455.	0.0	0.0	0.0	15.	0.0	0.0	0.0	29
0.133	26526.	0.0	0.0	0.0	15.	0.0	0.0	0.0	29
0.157	4216.	0.0	0.0	0.0	15.	0.0	0.0	0.0	29
0.182	-46273.	0.0	0.0	0.0	15.	0.0	0.0	0.0	29
0.184	-3624.	0.0	0.0	0.0	15.	0.0	0.0	0.0	29
0.175	-3734.	0.0	0.0	0.0	15.	0.0	0.0	0.0	29
0.191	6220.	0.0	0.0	0.0	15.	0.0	0.0	0.0	29
0.194	-3740.	0.0	0.0	0.0	15.	0.0	0.0	0.0	29
0.200	-3745.	0.0	0.0	0.0	15.	0.0	0.0	0.0	29
0.204	2088.	0.0	0.0	0.0	15.	0.0	0.0	0.0	29
0.214	340.	0.0	0.0	0.0	15.	0.0	0.0	0.0	29
0.221	4107.	0.0	0.0	0.0	15.	0.0	0.0	0.0	29
0.10.	0.0	0.0	0.0	0.0	15.	0.0	0.0	0.0	29
									9930

Figure 14. Input for Large Car.

INPUT HEAD BY CALSVA

6451	4448	905	0.0	0.25	70.	0.0	0.0	0.0	-1.0	1	
492	59.0	714	300.4	664.	17352.	19128.	0.0	0.0	330.	3	
94	5	56.7	56.3	8.81	8.67	0.5	0.0	-150.	6000.	4	
112.	15		3.23	58.	0.01	165012.	0.0	14.		5	
1098.	1.	10.	5.1	97.	0.01	112758.	0.0	36.03	-059.	6	
0.0	0.0	0.0	0.0	0.0	2.2	0.0	0.0	0.0	5200.	7	
0.0	0.0	0.0	1000.04	0.0	0.0	0.0	0.0	0.0		8	
0.0	0.0	0.0	0.0	0.0	0.0	0.0	0.0	0.0		9	
5.	15.	1.	0.0	15.	-8.					11	
0.0	0.0	0.0	0.0	0.0	0.0	0.0	0.0	0.0		12	
PHIC(1),1-1.	11										
-5.700	-3.900		-2.450	-1.300	-0.400	0.300	0.600	0.300	-0.400	0.650	-1.300
300.	0.0000	0.523	10.0000	0.1	1.5					14	
0.0	0.0	0.0	0.0	78.	15.	0.0	0.0			17	
0.15	-0.731.	0.0	0.0	78.	15.	0.0	0.0			24	
-0.22	-1.930.	0.0	250.	78.	15.	0.0	0.0			29	
-0.3	-1.446.	0.0	600.	78.	15.	0.0	0.0			29	
-0.39	-0.32.	0.0	1350.	78.	15.	0.0	0.0			29	
-0.47	-0.574.	0.0	2000.	78.	15.	0.0	0.0			29	
-0.58	-0.24.	0.0	3100.	78.	15.	0.0	0.0			29	
-0.66	-1.2831.	0.0	4300.	78.	15.	0.0	0.0			29	
-0.75	-0.257.	0.0	4600.	78.	15.	0.0	0.0			29	
-0.85	-1.257.	0.0	4800.	78.	15.	0.0	0.0			29	
-0.91	-1.0901.	0.0	5200.	78.	15.	0.0	0.0			29	
0.07	-1.1578.	0.0	5500.	78.	15.	0.0	0.0			29	
0.1	-1.1012.	0.0	4250.	78.	15.	0.0	0.0			29	
0.109	-1.3855.	0.0	3700.	78.	15.	0.0	0.0			29	
0.13	36.59.	0.0	3550.	78.	15.	0.0	0.0			29	
0.147	9.216.	0.0	3300.	78.	15.	0.0	0.0			29	
0.158	-6.272.	0.0	3000.	78.	15.	0.0	0.0			29	
0.164	-56.24.	0.0	2900.	78.	15.	0.0	0.0			29	
0.171	-37.44.	0.0	2790.	78.	15.	0.0	0.0			29	
0.181	0.20.	0.0	2560.	78.	15.	0.0	0.0			29	
0.194	-3760.	0.0	2300.	78.	15.	0.0	0.0			29	
0.209	-3765.	0.0	0.0	78.	15.	0.0	0.0			29	
0.24	2688.	0.0	0.0	78.	15.	0.0	0.0			29	
0.27	4109.	0.0	0.0	78.	15.	0.0	0.0			29	
0.0	0.0	0.0	0.0	78.	15.	0.0	0.0			29	
0.0	0.0	0.0	0.0	78.	15.	0.0	0.0			29	

Figure 15. Input for Medium Car.

minor variables which were not covered in the referenced work.

An examination of Figure 15 also reveals that the impulse input card series is that for the base-bending signpost model, highlighted by the inclusion of vertical as well as horizontal forces. Also, comparing Figure 14 (p. 46) and Figure 15 will show that the bumper position has moved closer to the vehicle center of gravity from the large to the medium car, as expected.

Compact car. Another well-documented vehicle, the compact car input data was easily compiled (2). Shown in Figure 16, the data is that for a 1971 Chevrolet Vega sport coupe, the same basic vehicle as that used for the crash tests covered previously. All variable values had been determined, so input presented no problem. Figure 16 also presents the base-bending signpost impulse data, and a quick comparison with Figure 15 will support the fact that the impulse data is identical in each signpost model, regardless of vehicle size.

Subcompact car. Presenting a final problem, the subcompact car data was the hardest to find. Eventually, a source containing the most important vehicle parameters was found (9). As with the medium car, the rest of the required input data had to be obtained from the next largest vehicle. Although more Vega data were required for the subcompact (a 1976 Honda Civic) than had been required for the medium car, the crucial and most influential data were found for the Honda, so the Vega values were merely supplemental and had little, if any, effect on the final results. Figure 17 is a listing of the subcompact input for the HVOSM, also showing the same breakaway model impulse data as presented in Figure 14 (p. 46) for the large car. As before, the bumper

INPUT READ BY CALSVA										
5.83	2.24	.002	0.0	.025	70.000	0.0	0.0	0.0	1.0	1
61.87	51.13	575	366.6	1838	72500.	18500.	1189.	11.83	323.	2
121.	6.	10.	2.	37.	7.01	0.21	36.	0.01	0.0	3
1240.	6.	10.	7.711	2364.	1.55	11690.	0.75	0.0	0.0	4
0.0	0.0	0.0	1080.64	0.0	0.0	0.0	0.0	0.0	0.0	5
0.0	-15.	-8.	0.0	15.	-8.	0.0	0.0	0.0	0.0	6
-4.	4.	1.	0.0	0.0	0.0	0.0	0.0	0.0	0.0	7
PHIC(1)=1.9										
-4.750 -3.080 -1.750 -0.730 0.0 0.480 0.650 0.780 0.830										
300.	0.000.	0	1000000.	.01	1.5	0.0	0.0	0.0	0.0	19
0.15	-97.31	0.0	0.0	73.	12.	0.0	0.0	0.0	0.0	20
-0.22	-1920.	0.0	250.	73.	15.	0.0	0.0	0.0	0.0	21
-0.39	-1486.	0.0	600.	73.	15.	0.0	0.0	0.0	0.0	22
-0.47	-6432.	0.0	1358.	73.	15.	0.0	0.0	0.0	0.0	23
-0.58	-9574.	0.0	2000.	73.	15.	0.0	0.0	0.0	0.0	24
-0.66	-5424.	0.0	3100.	73.	15.	0.0	0.0	0.0	0.0	25
-0.75	-12831.	0.0	4300.	73.	15.	0.0	0.0	0.0	0.0	26
-0.85	-6425.	0.0	4600.	73.	15.	0.0	0.0	0.0	0.0	27
-0.91	-10901.	0.0	5200.	73.	15.	0.0	0.0	0.0	0.0	28
PHIC(2)=1.9										
-4.750 -3.080 -1.750 -0.730 0.0 0.480 0.650 0.780 0.830										
0.97	-11528.	0.0	5500.	73.	15.	0.0	0.0	0.0	0.0	29
1.01	-11015.	0.0	5500.	73.	15.	0.0	0.0	0.0	0.0	30
1.04	-13855.	0.0	4250.	73.	15.	0.0	0.0	0.0	0.0	31
1.33	3659.	0.0	3700.	73.	15.	0.0	0.0	0.0	0.0	32
1.39	364.	0.0	3550.	73.	15.	0.0	0.0	0.0	0.0	33
1.47	4216.	0.0	3500.	73.	15.	0.0	0.0	0.0	0.0	34
1.58	-6272.	0.0	3300.	73.	15.	0.0	0.0	0.0	0.0	35
1.64	-3674.	0.0	3000.	73.	15.	0.0	0.0	0.0	0.0	36
1.71	-3748.	0.0	2900.	73.	15.	0.0	0.0	0.0	0.0	37
1.75	-734.	0.0	2790.	73.	15.	0.0	0.0	0.0	0.0	38
1.81	6220.	0.0	2500.	73.	15.	0.0	0.0	0.0	0.0	39
1.88	-3780.	0.0	0.0	73.	15.	0.0	0.0	0.0	0.0	40
1.94	-730.	0.0	0.0	73.	15.	0.0	0.0	0.0	0.0	41
2.00	2465.	0.0	0.0	73.	15.	0.0	0.0	0.0	0.0	42
2.14	580.	0.0	0.0	73.	15.	0.0	0.0	0.0	0.0	43
2.21	4109.	0.0	0.0	73.	15.	0.0	0.0	0.0	0.0	44
2.27	0.0	0.0	0.0	73.	15.	0.0	0.0	0.0	0.0	45
3.0.	0.0	0.0	0.0	73.	15.	0.0	0.0	0.0	0.0	46
9900										

Figure 16. Input for Compact Car.

INPUT READ BY CALSVA

3.11	2.494	.005	0.0	.025	70.	0.0	0.0	-1.0	1
32.11	54.89	.311	386.4	1756.	4457.	2698.	0.0	250.	3
125.05	5	51.	50.	8.49	8.49	1.3	-100.	5200.	4
105.75	5		3.59	37.	.001	0.0	11.		5
1240.	6.	10.	9.06	58.	.001	10500.	35.	-0.01	6
0.0	0.0	0.0	3.8	1800.	1.9	.5	.75	3400.	7
-4.	-15.	-8.	0.9	0.0	0.0	0.0	0.0		8
	1.		1080.64	15.	-8.				9
			0.0						11
									12
PHIC(1)=1.	9								
-4.750	-3.080		-1.750	-0.730	0.0	0.480	0.650	0.780	0.830
300.	0	.614	1000000.	.01	15	0.0			14
0.0	0.0	0.0	0.0	65.	15.	0.0			17
.015	-9731.	0.0	0.0	65.	15.	0.0			20
.022	-1930.	0.0	0.0	65.	15.	0.0			22
.03	-14486.	0.0	0.0	65.	15.	0.0			29
.039	-6432.	0.0	0.0	65.	15.	0.0			29
.047	-9574.	0.0	0.0	65.	15.	0.0			29
.058	-5424.	0.0	0.0	65.	15.	0.0			29
.066	-12831.	0.0	0.0	65.	15.	0.0			29
.075	-6425.	0.4	0.0	65.	15.	0.0			29
.085	-12507.	0.4	0.0	65.	15.	0.0			29
.091	-10901.	0.0	0.0	65.	15.	0.0			29
.097	-11528.	0.0	0.0	65.	15.	0.0			29
.101	-11015.	0.0	0.0	65.	15.	0.0			29
.109	-13835.	0.0	0.0	65.	15.	0.0			29
.133	3659.	0.0	0.0	65.	15.	0.0			29
.139	3644.	0.0	0.0	65.	15.	0.0			29
.147	4216.	0.0	0.0	65.	15.	0.0			29
.158	-6272.	0.0	0.0	65.	15.	0.0			29
.164	-3624.	0.0	0.0	65.	15.	0.0			29
.171	-3748.	0.0	0.0	65.	15.	0.0			29
.175	-734.	0.0	0.0	65.	15.	0.0			29
.181	6120.	0.0	0.0	65.	15.	0.0			29
.188	-3780.	0.0	0.0	65.	15.	0.0			29
.194	-730.	0.0	0.0	65.	15.	0.0			29
.200	2485.	0.0	0.0	65.	15.	0.0			29
.219	698.	0.0	0.0	65.	15.	0.0			29
.221	4109.	0.0	0.0	65.	15.	0.0			29
.227	0.0	0.0	0.0	65.	15.	0.0			29
10.	0.0	0.0	0.0	65.	15.	0.0			29

Figure 17. Input for Subcompact Car.

continued to move closer along the vehicle x-axis to the vehicle center of gravity as the car size decreased, but the 15 inches right of center offset of the force application was maintained.

### Conclusion

Approaching the parameter study with the necessity of credible results in mind, the input had to be reliable for the output to present a realistic approximation of actual signpost impacts. The signpost impulse data sets were developed, one for a breakaway model signpost, and the other for a base-bending signpost model. The input for the vehicle data was developed from the best available data for each of the car sizes: large, medium, compact, and subcompact. With the preparation of the input data, each of the four vehicle sizes were prepared for simulated impact with each of the signpost models.

At this point, the modified HVOSM was put into operation to compute the results of each of the eight separate vehicle cases. Analysis and presentation of those results was the final step of the thesis.



CHAPTER V  
PARAMETER STUDY RESULTS

Introduction

Modifying the HVOSM, validating the changed program, and assembling data necessary to evaluate AASHTO signpost standards culminated in the results shown in this chapter: the reactions of different sized automobiles in collisions with each of two different signpost configurations. Points of interest are not only whether the effect of the same signpost is markedly different on decreasing sizes of vehicles, but also how different methods of ground connection for the signpost (breakaway versus base bending) affect the same vehicle in a collision.

Parameter study results will be delineated in three major categories: the longitudinal acceleration of the sprung mass center of gravity, the vertical acceleration of the sprung mass center of gravity, and the vehicle travel path after impact. Center of gravity accelerations are a measure of the accelerations felt by the occupants of the vehicle, while the vehicle travel path is an indication of post-impact stability of the vehicle.

Before the separate results are presented, a quick view of the overall results will help to keep the major trends in focus. First of all, as expected, the changes in momentum were all in accordance with AASHTO specifications with one exception: the subcompact vehicle, when impacted with the base-bending signpost model, measured 1385 pound-seconds of momentum change, 26% above AASHTO standards. In this instance, the subcompact rolled over, even though the same impulse did

not affect the larger three cars, in terms of change in momentum or in terms of vehicle motion, nearly as severely. As anticipated at the outset of the thesis, the subcompact experienced extreme accelerations and one rollover in tests with the two signpost models.

#### Longitudinal Acceleration

The longitudinal acceleration of the sprung mass center of gravity was measured as an indication of the front-to-rear accelerations experienced by the vehicle passengers. The accelerations were measured only for the duration of the impact (up to .25 seconds), since they were negligible after that period of time. Generally, the maximum deceleration for each vehicle size was only slightly less for the base-bending model than for the breakaway model. Also, the maximum deceleration, as expected, increased for each decreasing vehicle size, almost doubling between the compact and subcompact vehicle sign impact simulations.

Large car. The large car accelerations are shown in Figure 18. The maximum deceleration is only 3.45 G's, experienced in the breakaway model of signpost impact. The values for the two different signpost models are in almost exact agreement for the first .16 seconds. After that, however, the acceleration values are small and the differences between the acceleration curves would not have an appreciable affect on the passengers, apart from the slightly greater decelerations experienced in the base-bending model.

Medium car. The medium car accelerations are shown in Figure 19. Graphed to the same scale as the large car accelerations shown in

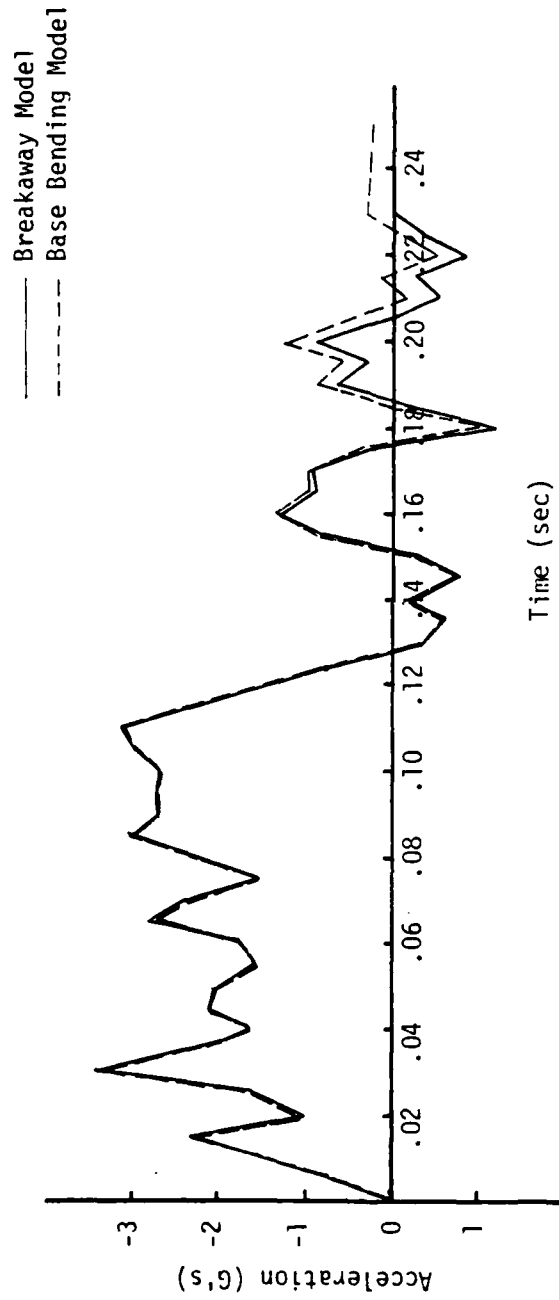


Figure 18. Sprung Mass C.G. Longitudinal Acceleration for Large Car.

— Breakaway Model  
- - - Base Bending Model

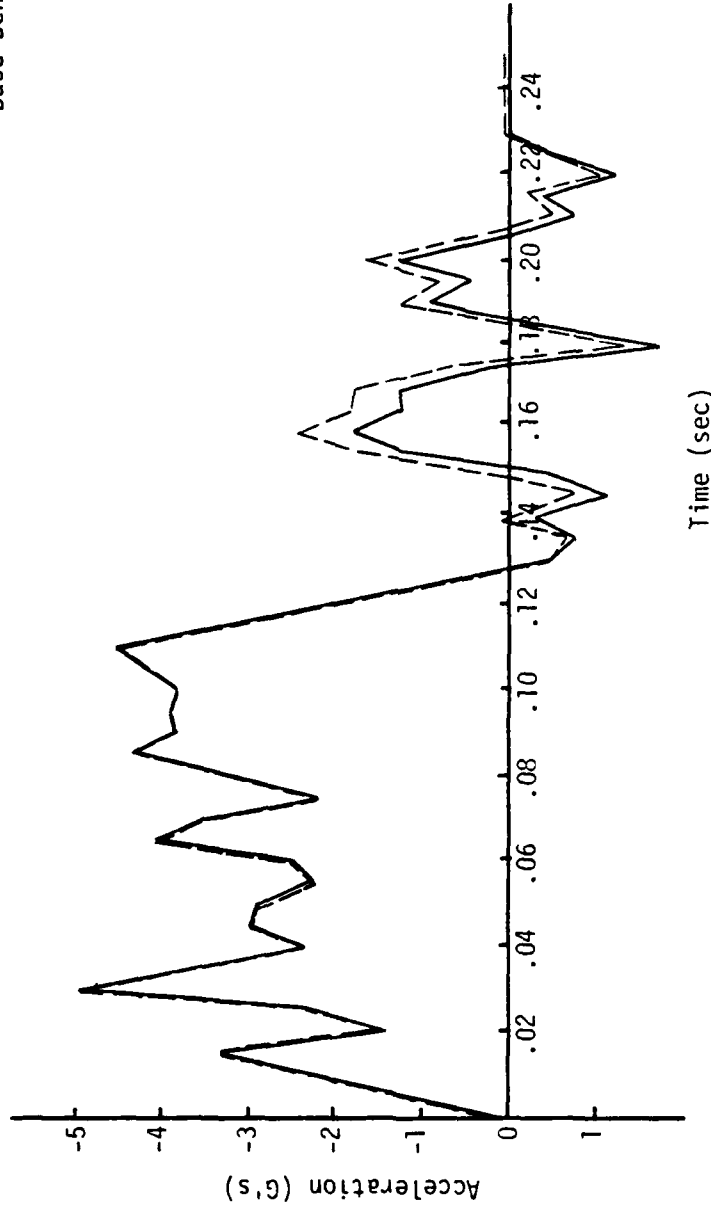


Figure 19. Sprung Mass C.G. Longitudinal Acceleration for Medium Car.

Figure 18, the maximum negative acceleration has increased to 5 G's, again for the breakaway model of sign impact. As before, the accelerations are in close agreement for the two sign impact models, separating only after .13 seconds into the collision. As with the large car, the base-bending model of signpost collision ends up causing greater decelerations than the breakaway model at the later stages of the collision. While the shape of the acceleration curve is similar to that for the large car, the magnitudes are greater overall for the medium car, and the larger accelerations and rapid reversals would be more noticeable to the vehicle passengers.

Compact car. Presented in Figure 20, the compact car accelerations are greater than those for the medium car at all points, much like a larger version of the same graph. Increasing to 5.49 G's, the maximum negative acceleration is experienced in simulated impact with the breakaway model signpost. As before, the breakaway and base-bending models match accelerations for .13 seconds, after which the base-bending model is associated with greater deceleration than the breakaway model. The accelerations, while greater in magnitude than those for the medium car, are not relatively that much larger than those for the medium car, so the effects on the vehicle would be only slightly greater.

Subcompact car. The differences between the accelerations of the subcompact car and the three larger vehicles are of such magnitude that the scale of the graph had to be increased. Shown in Figure 21, the acceleration scale is double the scale that was used for the three larger vehicles. While it appears to be the same as that for the compact car, the graph of the accelerations of the subcompact car is

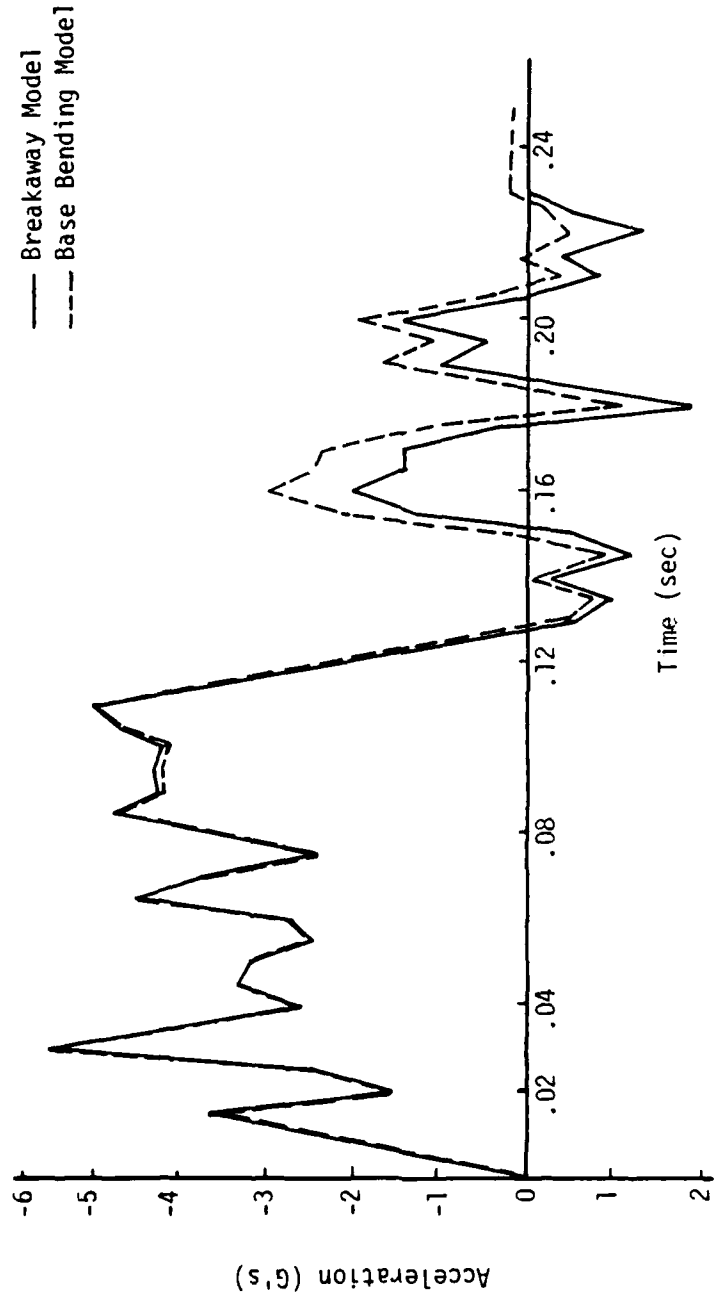


Figure 20. Sprung Mass C.G. Longitudinal Acceleration for Compact Car.

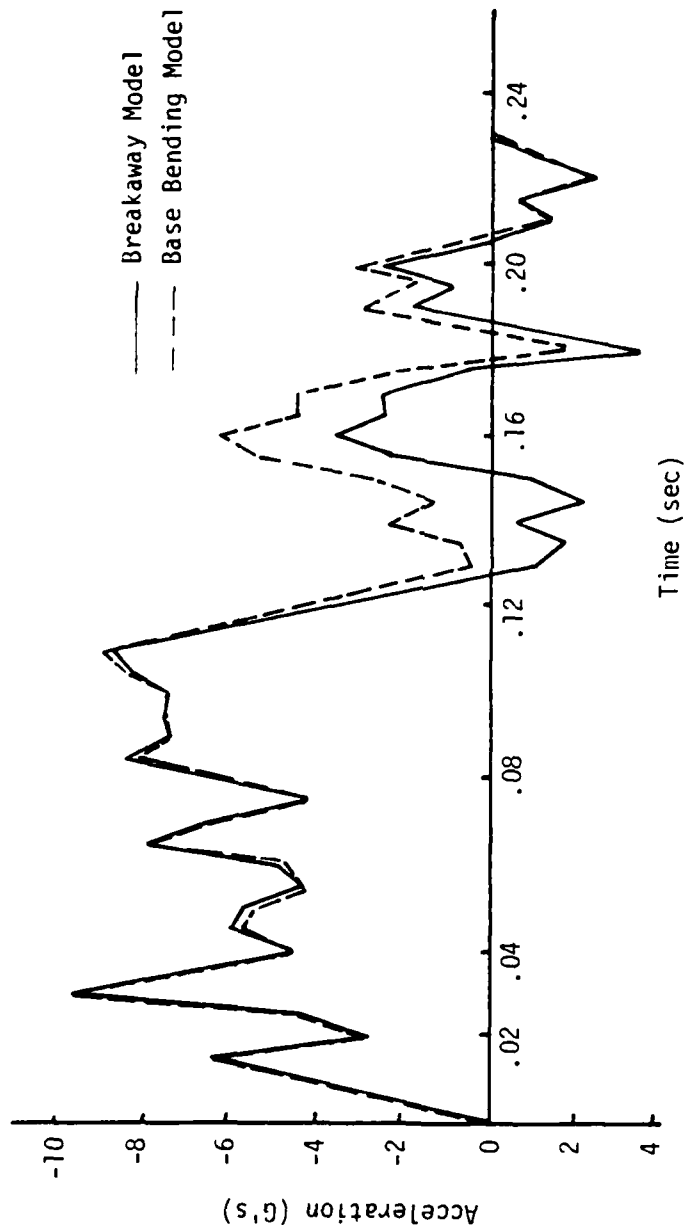


Figure 21. Sprung Mass C.G. Longitudinal Acceleration for Subcompact Car.

actually almost twice the magnitude. Another significant change is found in the difference between the accelerations experienced under the two sign models in Figure 21. Starting at .09 seconds after impact, the base-bending signpost model causes much greater decelerations by the vehicle than the breakaway model does. A maximum negative acceleration of 9.59 G's, as experienced in the breakaway model, is almost double the maximum of the compact car and almost triple that of the large car. While all accelerations are for short durations, the passengers in the subcompact car would be in much greater danger from deceleration effects than they would be in any of the three larger vehicles. As previously mentioned, rollover occurs in the base-bending model simulation for the subcompact, but the high accelerations experienced in the breakaway model, even without rollover, are hazardous.

In brief, the front-to-rear accelerations of the vehicles increase in magnitude as the car size decreases. While all accelerations are of short duration, they are so markedly greater for the subcompact car as to render its collision effects on the vehicle passengers particularly undesirable relative to the accelerations experienced in any of the three larger vehicles. Also, the base-bending model accelerations agree closely with the breakaway model accelerations, differing after a period of time in the direction of larger decelerations of the vehicle. As the car size decreases, the deviancy between the sign model accelerations grows in magnitude and the deviancy begins a shorter time after impact.



### Vertical Acceleration

At the sprung mass center of gravity, the vertical accelerations were compiled as a measure of the up-and-down accelerations felt by the passengers of each vehicle during signpost impact. People have lower tolerances to head-to-toe accelerations than they have to chest-to-back accelerations, which are longitudinal accelerations in this study. Therefore, the vertical accelerations in these cases have as much importance in measuring vehicle safety as the longitudinal accelerations. These vertical accelerations were graphed for a period of .25 seconds, which was long enough to cover all the extreme acceleration values associated with the impacts. In general, while the breakaway signpost only produced vertical accelerations worthy of notice in the subcompact car test, the base-bending model signpost produced high vertical accelerations, especially in the smaller vehicles.

Large car. Shown in Figure 22, the graph of the accelerations experienced by the sprung mass center of gravity does not resemble the impulse input as the longitudinal accelerations resembled the horizontal impulse input. There is no graph of the accelerations produced in the breakaway model because the maximum acceleration of .033 G's would not show up on the graph. An interesting reaction is produced by the initial positive acceleration of the vehicle center of gravity, followed by high negative accelerations. Since the positive direction of acceleration is downward for the HVOSM vehicle (Appendix II), that means that the passengers would feel the seats drop away, then slam upwards and drop away again as the negative acceleration peak at .215 seconds occurs. While not critical in this case due to the constructive

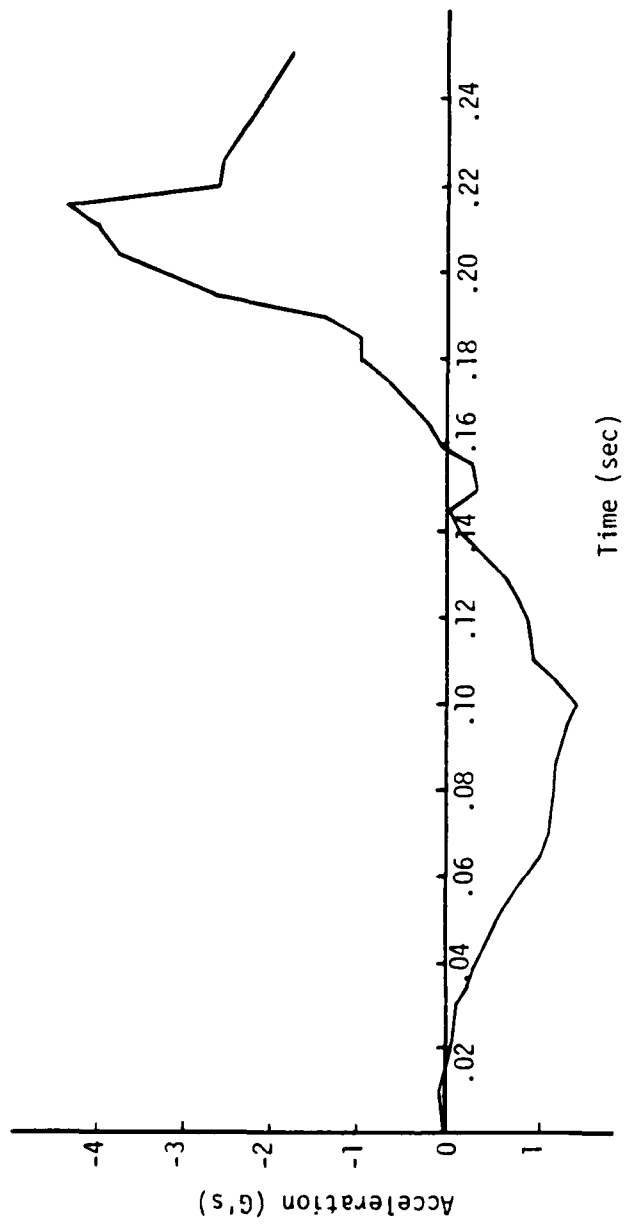


Figure 22. Sprung Mass C.G. Vertical Acceleration for Large Car in Base Bending Model.

effects of seatbelts and the almost instantaneous existence of the accelerations, these positive and negative accelerations grow in magnitude while acting in the same short time span as the car size decreases. As will be shown, the greater magnitudes and large reversals point to increasingly hazardous conditions, even with seatbelts and shoulder harnesses.

Medium car. Once again, the breakaway model fails to produce any significant vertical accelerations, with the maximum acceleration only reaching .09 G's. However, in the base-bending model signpost impact simulation, the maximum negative acceleration increases over 60% from that of the large car impact, as shown in Figure 23. As before, the initial downward acceleration is followed by rapid negative acceleration (upward), which then quickly drops off. These rapid reversals are the real danger since the other vehicle motions are not very extreme (as will be shown). Driver control becomes more difficult as these bounding motions become more violent.

Compact car. The sprung mass center of gravity vertical accelerations as recorded for the base-bending model sign impact are shown in Figure 24. At first glance the effects seem to be reduced, but the further increase in acceleration magnitudes caused the scale of accelerations to be doubled. So, the accelerations are really shown to half size of what they would be on the scale used for the medium and large cars. The usual downward acceleration followed by the large upward acceleration creates the same dangerous situation for the automobile occupants, and the maximum upward acceleration increased 10% over the maximum for the medium car. As with the two larger vehicles, there are

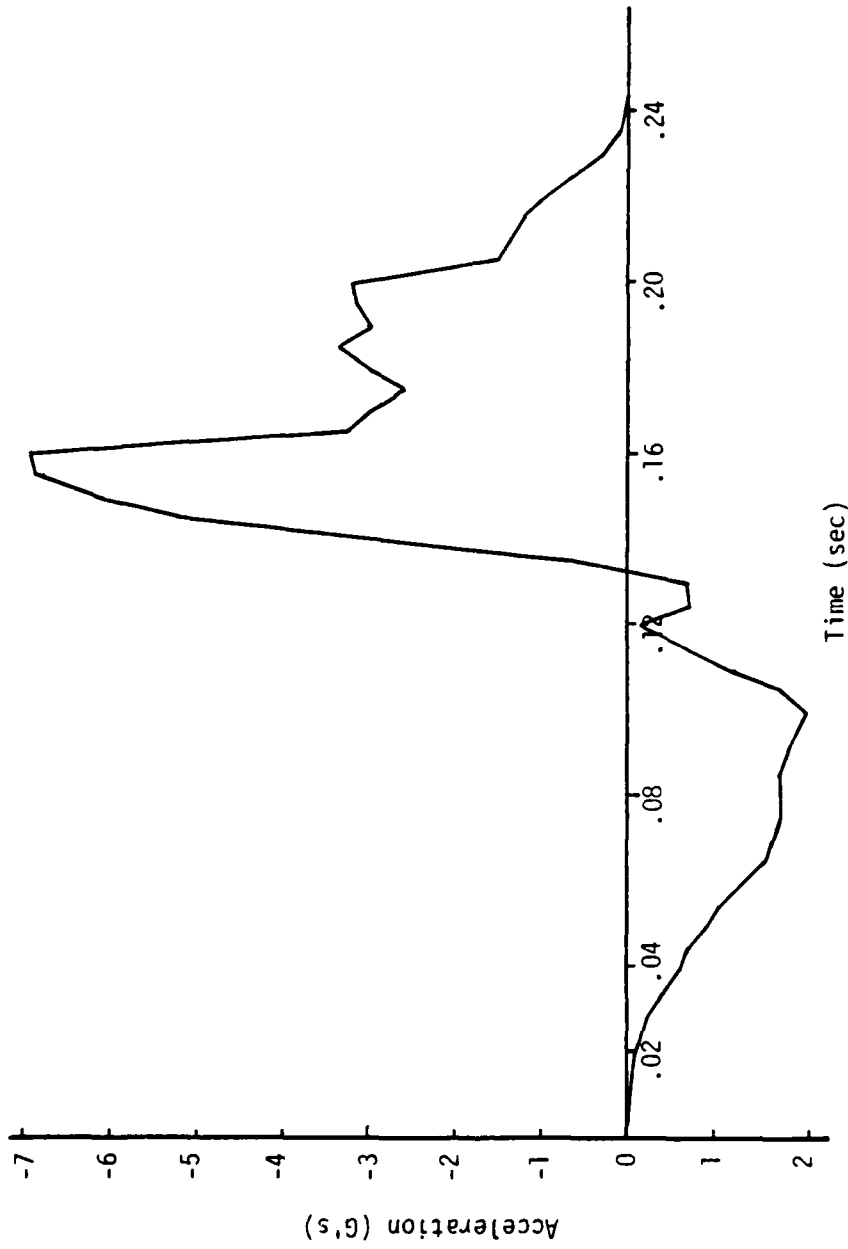


Figure 23. Sprung Mass C.G. Vertical Acceleration for Medium Car in Base Bending Model.

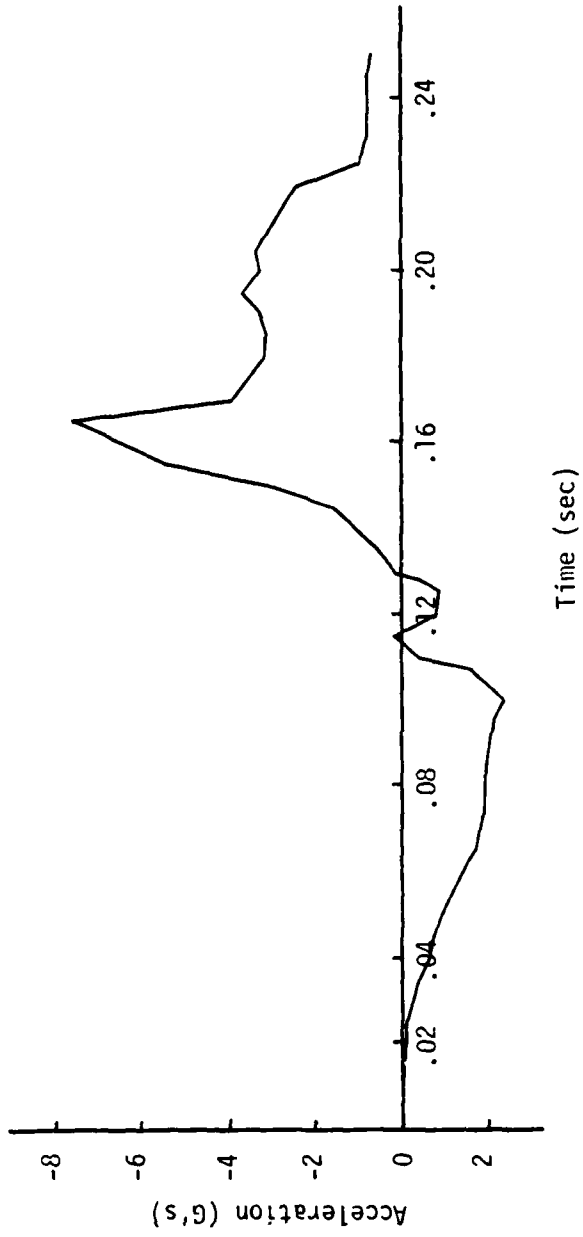


Figure 24. Sprung Mass C.G. Vertical Acceleration for Compact Car in Base Bending Model.

not any significant vertical accelerations produced in the breakaway model signpost impact.

Subcompact car. Shown on the same scale as those for the compact car (making the accelerations appear only half as large as they would be on the scale used for the medium and large cars), the accelerations of the vehicle under both signpost models appear in Figure 25. The breakaway model produces larger vertical accelerations for the subcompact car than for any of the other car sizes, but even the accelerations experienced in this case are negligible and do not present a hazard, especially relative to any of the accelerations experienced in the base-bending model of signpost impact. For an idea of the magnitude of the maximum negative acceleration for the subcompact in the base-bending model, the value is 3.5 times the maximum experienced by the large car and twice as large as that for the compact car. The base-bending model, it must be remembered, causes rollover of the subcompact, but the high vertical accelerations would probably render the vehicle occupants incapable of noticing the vehicle rollover. The vertical accelerations caused by the base-bending model on the subcompact are even greater than the maximum longitudinal acceleration (for which the body has a higher tolerance).

As was the case with the longitudinal accelerations, the vertical accelerations of the vehicle increase in magnitude as the vehicle size decreases. Under the base-bending model impact, the maximum vertical acceleration is greater than the maximum longitudinal acceleration. Unfortunately, the vertical accelerations affect the body more than the longitudinal accelerations. The breakaway model signposts produce the

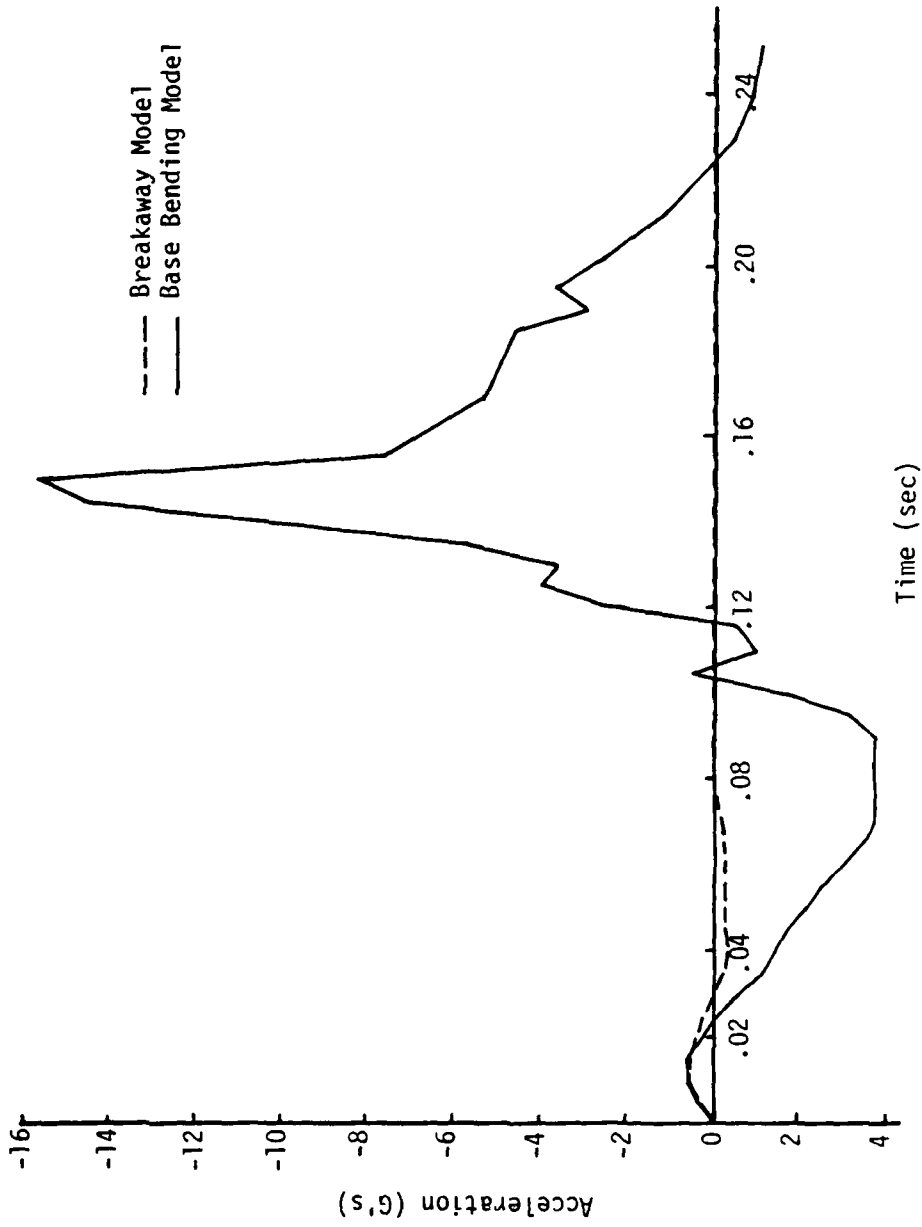


Figure 25. Sprung Mass C.G. Vertical Acceleration for Subcompact Car.

greatest longitudinal accelerations, but the model only produces noticeable vertical accelerations on the subcompact vehicle.

#### Travel Path

The lateral motion of the vehicle under a free steering mode gives an indication of the controllability of the vehicle after sign impact. The following graphs show both the path of the vehicle and an arrow at intervals to give an idea of the vehicle orientation as it travels after the signpost impact.

In presenting the vehicle paths, full use of each graph is made to present the information in an uncluttered manner. The side effect of this decision, however, is a great variance in scale of the lateral displacement of the vehicle. Therefore, the analysis below is made with an effort to keep the relative paths of each vehicle in perspective. Mainly, though, the problem is that the graphs cannot be compared without adjusting for scale when viewing them.

Vehicle stability after collision is measured by the possible controllability of the vehicle after signpost impact. For example, a car which, in the free steering mode, corrects itself smoothly to its pre-impact orientation is very stable; on the other hand, a wildly spinning car could not be controlled by any driver input, and thus the vehicle reaction is classified as unstable. Of course, any car which rolls over does not require a path analysis; the hazard is obvious.

Large car. Performing as expected, the large car is very stable in either sign model impact simulation. Shown in Figure 26, the break-away model sign impact results in a 10-foot displacement to the right



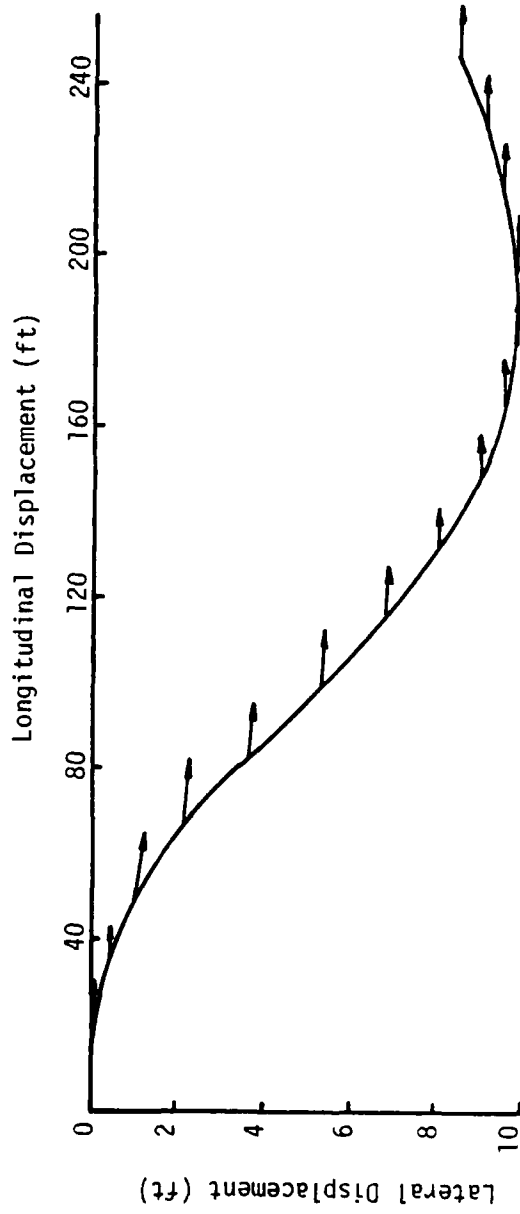


Figure 26. Path and Orientation of Large Car in Breakaway Model.

by the large car. Travelling smoothly, the car fishtails very slightly to the left at sign impact, correcting its own course during travel with subsequent steer to the left. On the same scale, the base-bending model sign impact vehicle motion is presented in Figure 27. Small steering angles result in only a 6-foot displacement to the right. Both vehicle paths could be easily controlled by any driver input, and the lateral travel distance of the vehicle relative to the "forward" travel of the vehicle is very small.

Medium car. Presented on two different lateral scales, the travel paths of the medium car show good stability. After impact with the breakaway signpost, the medium car steers wide right and then starts to overcorrect to the left as illustrated in Figure 28. While travelling 24 feet to the right, the vehicle can be easily controlled before the overcorrection to the left by the free steering vehicle takes place.

The base-bending signpost impact travel path, presented in Figure 29, is even more stable and has less lateral travel. The lateral travel of only 9 feet, compared to 24 feet for the breakaway signpost, places the travel path of the vehicle for the base-bending model impact very close to the original course compared to the breakaway model impact. However, a growing factor in the driver controllability is the effect of the longitudinal and vertical accelerations previously mentioned on the driver's ability to steer the car. While neither of the medium car impact models would incapacitate the driver, the following two car sizes demonstrate more hazardous outcomes, especially in the base-bending model impacts.

Compact car. As just stated, the high accelerations experienced

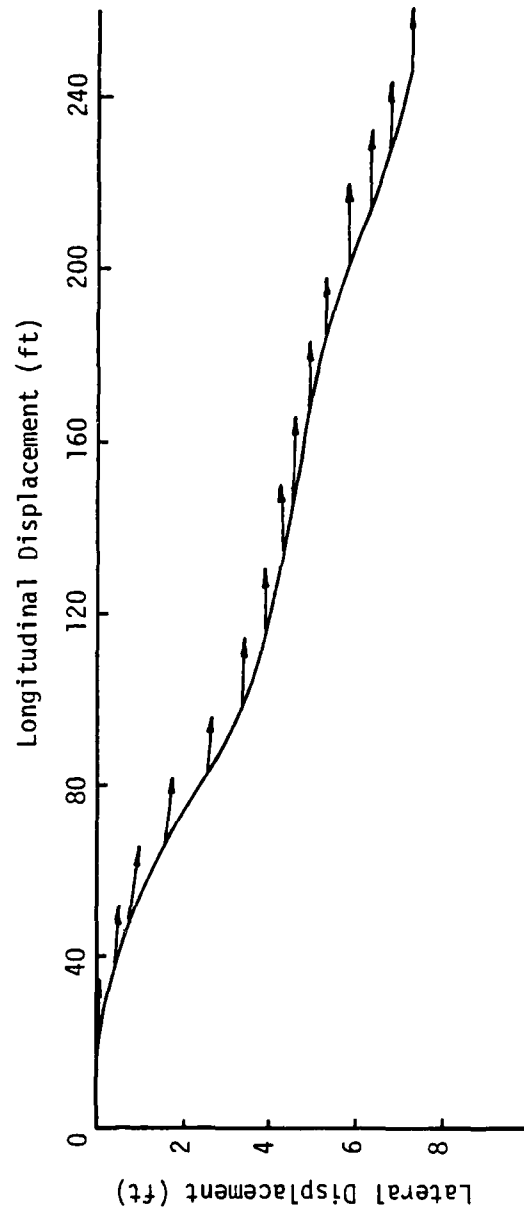


Figure 27. Path and Orientation of Large Car in Base Bending Model.

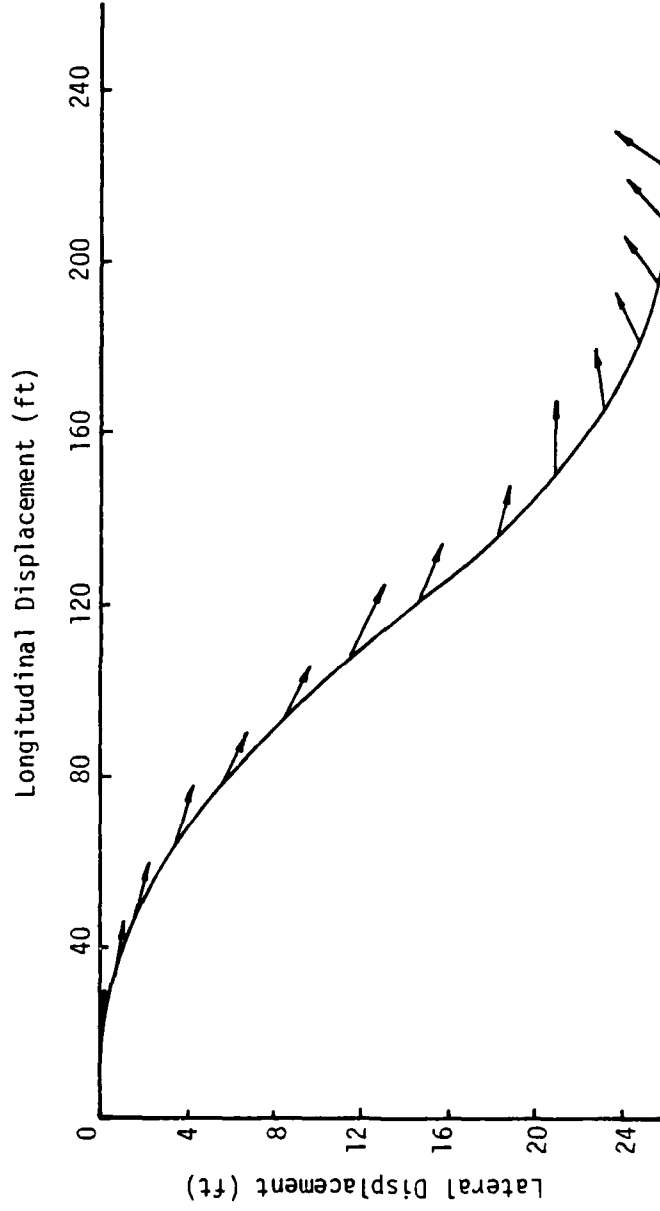


Figure 28. Path and Orientation of Medium Car in Breakaway Model

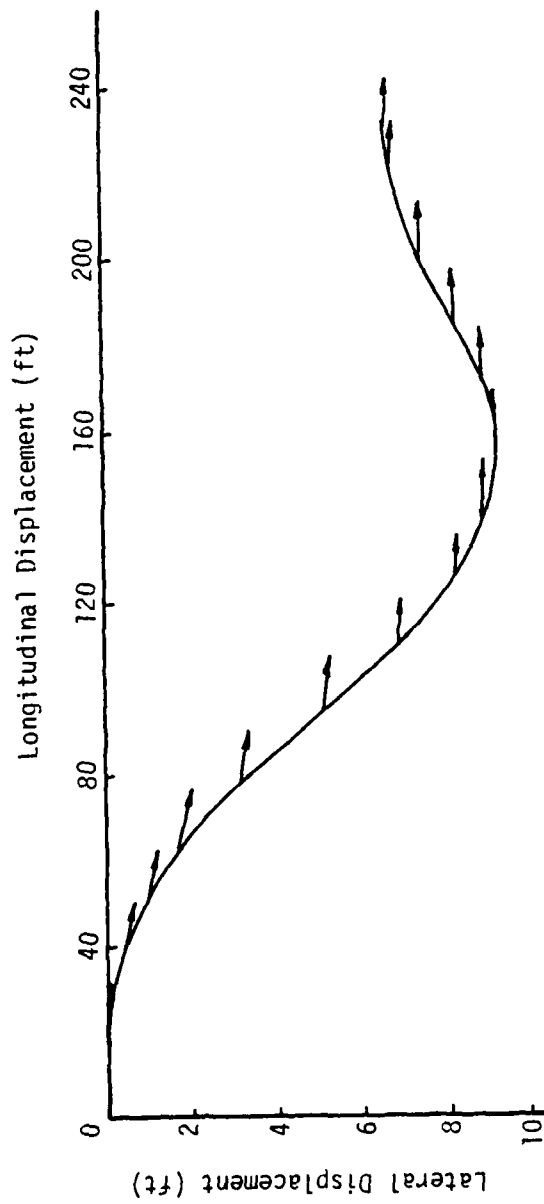


Figure 29. Path and Orientation of Medium Car in Base Bending Model.

in the vehicle collisions with the signpost models could have affected the driver's ability to steer the vehicle. But, just as the vehicle stability is getting more critical due to increasing driver hazard from accelerations, the vehicle stability decreases with decreasing vehicle size. As shown in Figure 30, the compact car impacts with the breakaway sign and fishtails gradually left until the vehicle is oriented at right angles to its original course. A lateral displacement of 50 feet is unsafe because other obstacles, such as fences, ditches, and embankments, exist along highways; and many of these obstacles are within 50 feet of the road shoulder. While the essentially longitudinal accelerations generated in the breakaway model impact would not incapacitate the compact car driver, the car is seen as marginally stable because of the excessive lateral travel and the need for control.

The base-bending model impact, on the other hand, produces a relatively small lateral displacement of 17 feet as seen in Figure 31. The vehicle corrects its own path, which is important because the vertical and longitudinal accelerations would almost certainly limit the driver's ability to control the path of the vehicle. As mentioned at the start, the scale differences between the travel path graphs along the lateral axis for the compact car are very great, and the lateral displacement of the compact car impacting the base-bending model signpost would be very small on the graph of the travel path for the breakaway signpost impact.

Subcompact car. Complete loss of stability is demonstrated in each signpost model collision simulation using the subcompact car. The breakaway model causes vehicle spinout, while the base-bending model

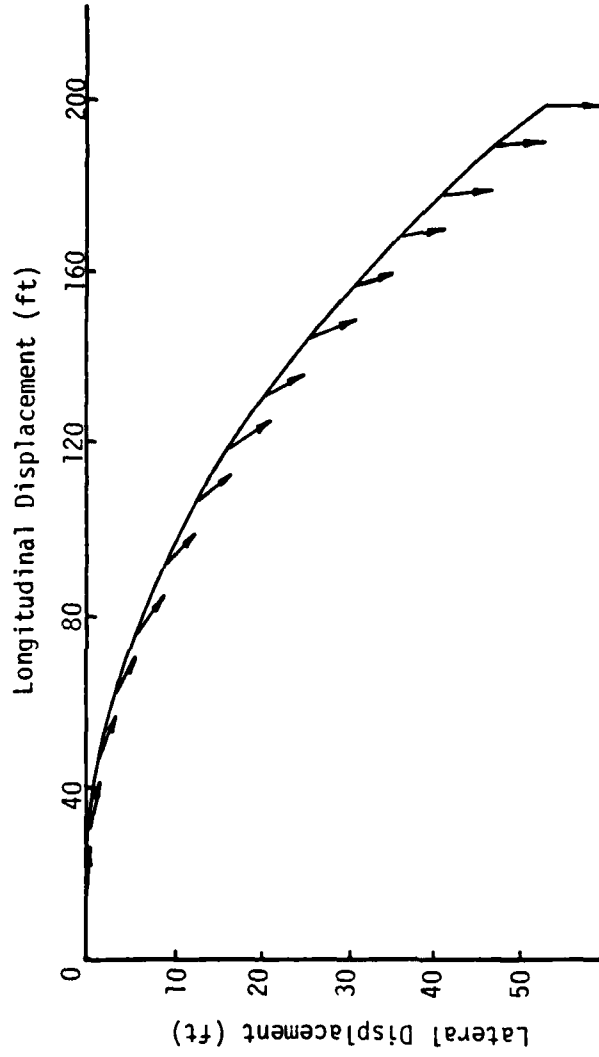


Figure 30. Path and Orientation of Compact Car in Breakaway Model.

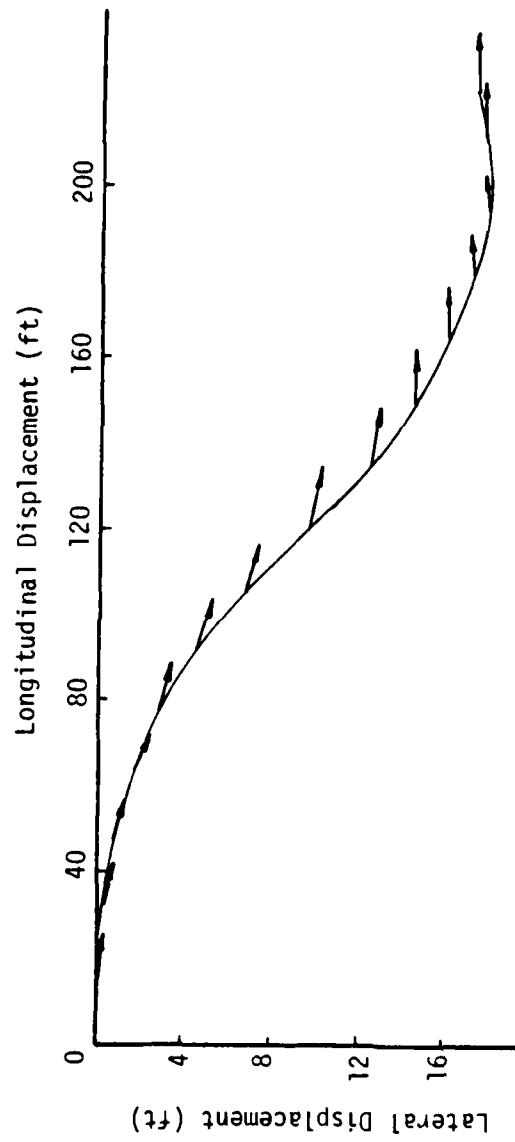


Figure 31. Path and Orientation of Compact Car in Base Bending Model.



impact results in vehicle rollover. No matter which signpost model is used, the vehicle path, when combined with the vehicle accelerations, prints only to extreme hazard. Presented in Figure 32, the path and orientation of the subcompact car subsequent to impact with the breakaway model signpost reveals the  $360^{\circ}$  spin and the relatively small lateral displacement of only 8 feet. That is the smallest breakaway model sign impact lateral displacement of the four vehicle sizes, and the main reason for the small lateral displacement is the rapid spin of the vehicle. No vehicle control is possible for the subcompact, but, after the large longitudinal accelerations experienced by the driver in the sign impact, there is not a high expectation of driver input after impact.

The limited results of the base-bending model impact are shown in Figure 33. The rollover is considered completed after a  $45^{\circ}$  roll angle is established. The rapid spinning of the vehicle prior to rollover is shown, along with the fractional lateral displacement. Effectively, in comparison with all other vehicle paths, the travel path prior to rollover for the subcompact in the base-bending model impact was quite similar to that of the large car in the base-bending model impact.

In general, the stability of the vehicle after signpost impact decreases with decreasing vehicle size, illustrated in this study by the total loss of control of the subcompact car. The base-bending model signpost impact tends to result in more stable motion and less lateral displacement than the breakaway sign impact. The increased stability of the base-bending model impact is offset by the higher longitudinal and vertical accelerations endured by the vehicle occupants.

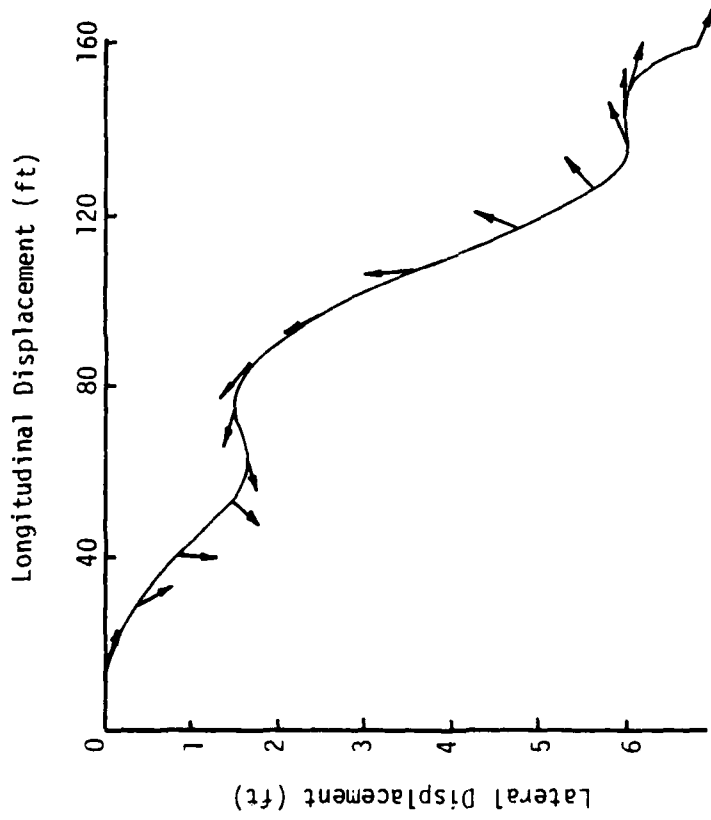


Figure 32. Path and Orientation of Subcompact Car in Breakaway Model.

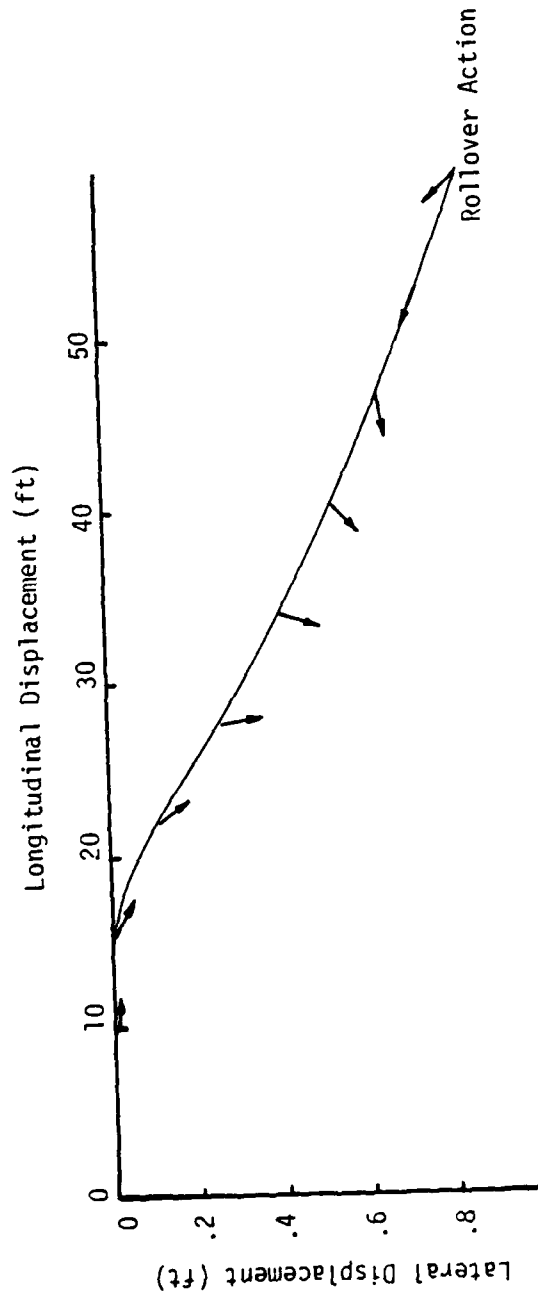


Figure 33. Path and Orientation of Subcompact Car in Base Bending Model.

### Summary

A compilation of the essential parameters of the study are gathered in Table 3. The different car sizes and their results in each of the two signpost model simulated impacts are presented for easy comparison and for review of the trends covered in this chapter.

First of all, the accelerations as measured at the sprung mass center of gravity, and thus approximately the same as those experienced by the vehicle occupants, increase as the car size decreases. The breakaway model signpost is associated with slightly larger longitudinal accelerations and insignificant vertical accelerations compared to those recorded in the base-bending model impacts. In each case, however, the maximum accelerations suffered by the subcompact are approximately double those of the compact car and triple those of the large car.

Secondly, the vehicle grows more unstable as the vehicle size decreases; this is compounded by the increased incapacity of the driver due to the increasing accelerations with decreasing vehicle size. The subcompact is totally unstable, experiencing spinout in the breakaway signpost impact and rollover in the base-bending model signpost impact. The same signpost that produces small pitch and yaw angles (shown in Table 3) in the compact vehicle is devastating to the subcompact in the base-bending model impact simulations. While the vehicle occupants were safer in the breakaway model impact of the subcompact, the surprising fact is this: The difference between installing a breakaway base support and simply driving the same signpost into the ground (base bending) in a collision by a subcompact vehicle is the difference between a survivable spinout and a possibly fatal vehicle rollover.

TABLE 3. Vehicle Sign Impact Results.

CAR SIZE	LARGE		MEDIUM		COMPACT		SUBCOMPACT	
	Break	Bend	Break	Bend	Break	Bend	Break	Bend
Signpost Model								
Change in Momentum ((lb-s)	1095.	1103.	1097.	1162.	1098.	1210.	1106.	1385.
Maximum Roll Angle (degrees)	-3.26	-8.1	3.33	-6.73	-5.86	-15.51	4.09	Rollover
Maximum Pitch Angle (degrees)	.12	8.54	.55	8.78	.38	17.25	-1.38	Rollover
Maximum Yaw Angle (degrees)	7.34	6.85	-55.0	14.07	90.+	23.09	360.+	Rollover
Maximum Longitudinal Acceleration (G's)	-3.45	-3.446	-4.999	-4.99	-5.493	-5.482	-9.591	-9.552
Maximum Vertical Deceleration (G's)	+0.033	-4.379	+0.09	-6.92	-.056	-7.671	-.561	-15.58
Weight (lbs)	4201.		2903.		2639.		1509.	

## CHAPTER VI

## CONCLUSION

As times change, standards must be kept up to date with technological breakthroughs and changing conditions which affect those standards. The recent trend in smaller, lighter cars brought about by the gas shortage and the use of plastics technology to decrease vehicle weight warranted the re-examination of signpost standards, especially in light of crash tests which indicated a hazard for light vehicles in signpost impacts (7). While the standards for signposts had been established in consideration of compact cars when compact cars were a small minority of road traffic, the growing percentages of compact and subcompact cars make roadside design for the smaller sizes a necessary concern.

To properly study the effects of a sign deemed safe by AASHTO standards on a range of car sizes, a dependable and valid computer simulation had to be used in order to obtain repeatable results. The best model, the HVOSM, was modified and validated to accept idealized sign impact data as generalized impulses. The three-dimensional capabilities of the modified HVOSM provided an excellent means to study the post-impact motions and their effects on the vehicle. Four vehicle sizes were used to cover the general vehicle categories: large, medium, compact, and subcompact. Two signpost models were created to represent the general installation methods: breakaway at the base, and base bending due to placement of the signpost into the ground as its own support.

The input for each vehicle and signpost model was made with

deliberate care to approximate real impact conditions. The impulses were generated to test the extremes of the AASHTO standards; that is, a 60 mile per hour impact with a signpost impacting an impulse of 1100 pound-seconds. The breakaway signpost was idealized as causing only horizontal impulses, while the base-bending model contained the same horizontal impulse plus a vertical impulse modeled after actual crash test results.

The results of the simulation confirm the expected results: The signposts which are safe for the larger cars have hazardous effects on the subcompact car. The breakaway sign impact results in spinout and excessively high accelerations for the subcompact, and the base-bending model impact causes even greater accelerations and eventual vehicle rollover. In each case, the base bending model of installation produces more hazardous effects for the vehicle occupants than the same signpost installed for breakaway action in impacts.

While these results definitely point to the need for re-examination of the AASHTO standards, they also point to an extension of these parameter studies. This parameter study was performed assuming ideal roadside conditions: flat, level terrain with a coefficient of friction between the tires and the surface of .5. Realistic roadside conditions would tend to magnify the hazards of impact with sideslope, shoulder roughness, and possible roadside ditches. The proposed new areas of investigation could be easily approached using the modified HVOSM, a proven simulator of signpost impact effects. Regardless of further studies, this thesis reveals that the AASHTO standards expose drivers of subcompact vehicles to dangerous sign impact effects even under the best of conditions.

## APPENDIX I

## REFERENCES

1. Basso, G. L., "Functional Derivation of Vehicle Parameters for Dynamic Studies," Report LTR-ST.747, Highway Safety Research Institute, National Research Council, Canada, September, 1974.
2. Deleys, N. J., and Segal, D. J., "Vehicle Redirection Effectiveness of Median Berms and Curbs," Report No. HF-5095-V-2, Calspan Corporation, Transportation Safety Department, Buffalo, N. Y., May, 1973.
3. James, M. E., Jr., and Ross, H. E., Jr., "HVOSM User's Manual," Research Report 140-9, Study 2-10-69-140, Texas Transportation Institute, Texas A&M University, August, 1974.
4. James, M. E., Jr., Ross, H. E., Jr., and Whittington, C., "Improvement of Accident Simulation Model," Report No. RF 3258-1, Texas A&M Research Foundation, Texas Transportation Institute, Texas A&M University, November, 1976.
5. McHenry, R. R., and Segal, D. J., "Determination of Physical Criteria for Roadside Energy Conversion Systems," CAL NO. VJ-2251-V-1, Buffalo, N. Y., July, 1967.
6. McHenry, R. R., and Deleys, N. J., "Vehicle Dynamics in Single Vehicle Accidents: Validation and Extensions of a Computer Simulation," CAL NO. VJ-2251-V-3, Buffalo, N. Y., December, 1968.
7. Ross, H. E., Jr., Walker, K. C., and Effenberger, M. J., "Crash Tests of Small Highway Sign Supports," Research Report 3254-3, Texas A&M Research Foundation, Texas Transportation Institute, Texas A&M University, January, 1979.
8. Segal, D. J., "Highway-Vehicle-Object Simulation Model--1976," Report No. FHWA-RD-76-165, Volumes 1-4, Office of Research & Development, Federal Highway Administration, Washington, D.C., February, 1976.
9. Shaw, L. M., "An Assessment of Performance of Impact Attenuators Mounted on Curbs," Contract DOT-FH-11-9287, Dynamic Science Inc., June, 1979.
10. "Standard Specification for Structural Supports for Highway Signs, Luminaires, and Traffic Signals," American Association of State Highway and Transportation Officials, 1975.
11. Young, R. D., Edwards, T. C., Bridwell, R. J., and Ross, H. E., Jr., "Documentation of Input for the Single Vehicle Accident Computer Program," Research Report 140-1, Texas Transportation Institute, Texas A&M University, July, 1969.



APPENDIX II  
A DESCRIPTION OF THE HIGHWAY-VEHICLE-OBJECT  
SIMULATION MODEL

The Highway-Vehicle-Object Simulation Model (HVOSM) is a mathematical model which can be utilized to investigate various problems associated with the roadway environment. It is used to study the dynamic behavior of an automobile under different roadway and roadside conditions. These conditions include such problems with the roadway environment as highway traffic barrier collisions, rapid lane change maneuvers, handling response on horizontal curves, drainage ditch cross sections, and now sign impacts.

The HVOSM was developed by Cornell Aeronautical Laboratory (CAL) (5,6) and later modified for specific program studies by the Texas Transportation Institute (TTI) (11). A conceptual idealization of the model is shown in Figure 34. The model is idealized as four rigid masses, which include: (a) the sprung mass ( $M_s$ ) of the body supported by the springs, (b) the unsprung masses ( $M_1$  and  $M_2$ ) of the left and right independent system of the front wheels, and (c) the unsprung mass ( $M_3$ ) representing the rear axle assembly.

The eleven degrees of freedom of the model include translation of the automobile in three directions measured relative to the fixed global coordinate system, rotation about the three local axes of the automobile, independent displacement of each front wheel suspension system, suspension displacement and rotation of the rear axle assembly, and steer of the front wheels. A further explanation of this model for in-depth analysis can be found by examining the references quoted

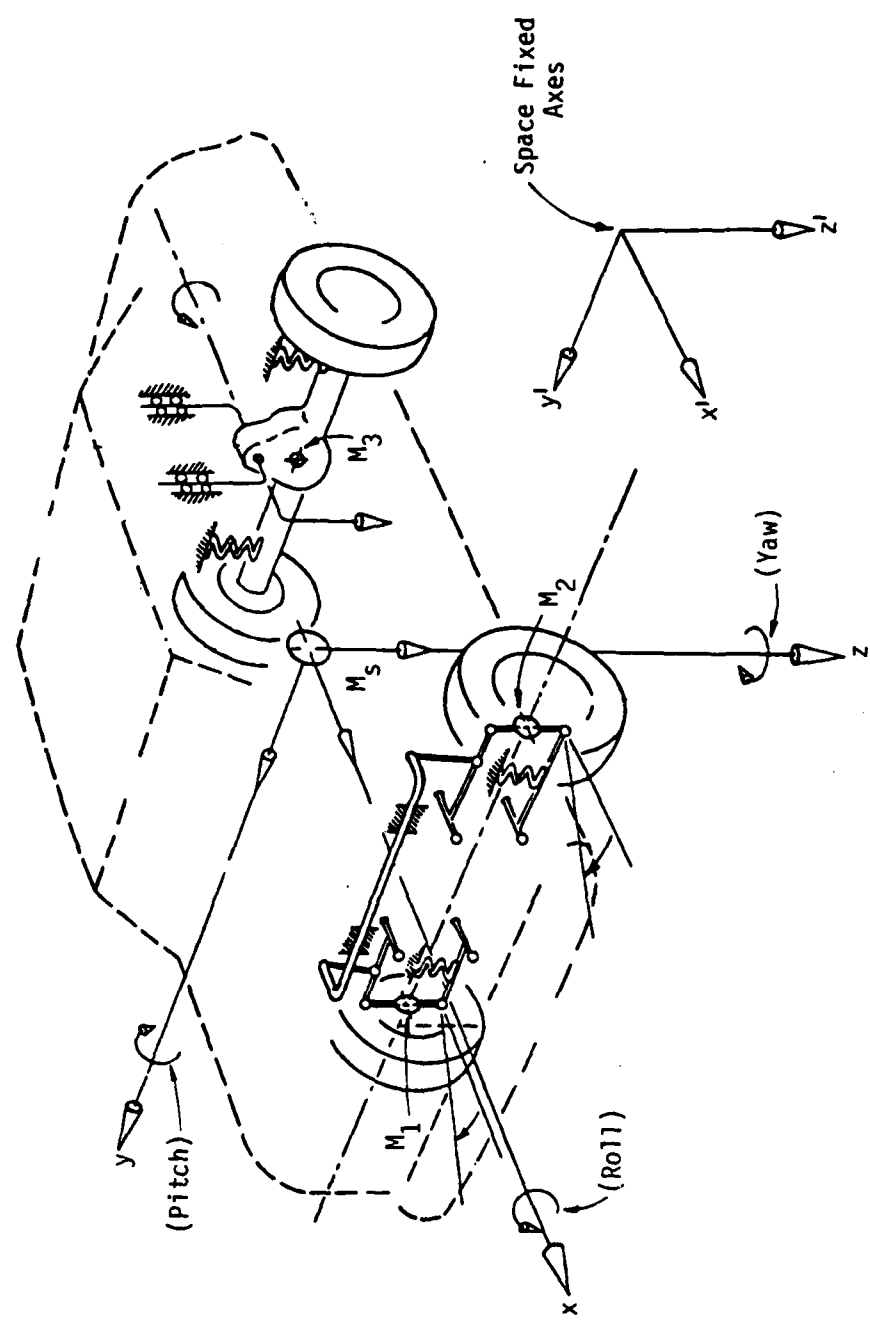


Figure 34. Idealization of Automobile.

earlier in this section, and also by examining Reference 8.

APPENDIX III  
CORRECTION OF ORIGINAL HVOSM FOR IBM 360 COMPUTER  
AND CURRENT FORTRAN H EXTENDED COMPILER

Introduction

The HVOSM program deck, which was the 1976 version stored in the files at Texas A&M University as supplied by CALSVA and modified by TTI, would not run without program error statements generated by the Fortran H extended compiler. The correction of these errors was very time consuming and frustrating, so this documentation will list the changes made in order to get the version to run prior to modification. The errors were of three basic types: subroutine name errors, EQUIVALENCE statement errors, and BLOCK DATA errors.

Subroutine Name Errors

When the HVOSM was written, the CLEAR subroutine, which is built into the computer system and not listed in the card deck, was used in the main program and the MATRIX subroutine to clear addresses in the common blocks. The assumed operation of subroutine CLEAR is that the parameter list contains the first and last addresses in the common block, and the computer clears all addresses between, and including, the two addresses given in the parameter list. The program would not run on the Texas A&M computer system because this subroutine, while it is listed in the computer system, is not the same one that the developers of the HVOSM used.

On the Texas A&M IBM 360, the subroutine ERASE is provided which uses the same parameter list and performs the same function that the

CLEAR subroutine did in the original program on whatever computer system CALSVA used. All that had to be done to correct this error was to replace the CLEAR subroutine call statements in MAIN and MATRIX with ERASE subroutine call statements -- a process of merely replacing the word CLEAR with the word ERASE.

#### EQUIVALENCE Statement Errors

This was by far the largest source of errors in the HVOSM program. When the program was originally written, the compiler would perform different functions than the present compiler in use at Texas A&M. The explanation of the reason for changes and the list of necessary changes is very simple, but the actual program changes were very numerous and time consuming. This explanation is intended to save a lot of time, and the action to clear up these errors results in a much neater and more compact program.

Using the older compiler systems, an equivalence could be made between a matrix and a certain series of variables quite easily. For example, the matrix A(4) and the variables A1, A2, A3, and A4 could use the following EQUIVALENCE statement:

```
EQUIVALENCE(A,A1)
```

This statement would automatically set A(1) equal to A1, A(2) equal to A2, and so on until the limits of the matrix were met. This operation was possible because the EQUIVALENCE statement took the first variable of a numerical sequence and set the equivalence between the first matrix location and the variable listed, and then automatically set the equivalence for the same number of following addresses in the common block as there were in the matrix. In another example, two equally

sized matrices could be set equal to each other with a single EQUIVALENCE statement. If the matrices were named ONE and TWO, the computer would equate the values in similar locations of each matrix so that they were identical by the use of the following command:

```
EQUIVALENCE(ONE,TWO)
```

The computer compilers at Texas A&M, however, do not allow these two operations. Each EQUIVALENCE statement must have a one-to-one correspondence between variables listed in the statement, which requires the filling of each separate location of matrices. So, in the past it was easier to link several different subroutines and their individual variables using EQUIVALENCE statements and matrices. Now, however, it is easier and also neater to scrap all duplicate variables so that one program variable is used throughout the program.

The following list of EQUIVALENCE statements which had to be repaired are accompanied by an explanation of the program surgery used to repair the errors. All of the listed EQUIVALENCE statements were deleted from the program after they were replaced by the new EQUIVALENCE statements or they were rendered useless by the elimination of one of the variables in each set. All changes were made to the program to affect the least number of equations, and all "series" variables like A1, A2, A3, and A4 were replaced by the simpler matrix form.

```
EQUIVALENCE(YCIP,YCIP)
```

The change was: YCIP was replaced by YCIP(1), and YC2P was replaced by YCIP(2). The common block INPT1 was changed by replacing "YCIP, YC2P," with "YCIP(2)," and the DIMENSION statement for YCIP was then deleted. Then, all the YCIP and YC2P locations were replaced by YCIP(1) and YCIP(2), respectively.

EQUIVALENCE(XP,X1P),(YP,Y1P),(ZP,Z1P),(PHII,PHI1),  
(PSII,PSI1),(UI,U1),(VI,V1),(WI,W1)

This statement was corrected by the lengthy procedure of replacing X1P through X4P with XP(1) through XP(4) throughout the whole program. All of the XP, YP, ZP, PHII, PSII, U, V, and W matrices are one-dimensional and four addresses long. So, in like manner, Y1P to Y4P, Z1P to Z4P, PHII to PHI4, PSI1 to PSI4, U1 to U4, V1 to V4, and W1 to W4 were replaced by YP(4), ZP(4), PHII(4), PSII(4), UI(4), VI(4), and WI(4), respectively, with the variable numbers matching the matrix address locations in each case.

The common blocks were also changed to reflect these improvements. DIMV common block was modified so that XP(4), YP(4), ZP(4), PHII(4), and PSII(4) replaced the previously listings of the variables X1P to X4P, Y1P to Y4P, and so on. All of the equations in which any of the phased out variable names were listed were changed to reflect the new matrix names and locations. The common block ADTNL was modified so that UI(4), VI(4), and WI(4) replaced the previous listings of U1 to U4, V1 to V4, and W1 to W4. Those equations had to be changed for the new matrix names and locations, also.

Special caution had to be used in subroutine DRIVER, where the variable PSI1 was used in the parameter list. In the DRIVER subroutine, the variable names for PSI1 were changed to PSII, but were not subscripted with a matrix location because the parameter list would not accept a matrix location, and also because it was a local subroutine variable and not used in the normal program sense in that subroutine.

After all of this was performed, the DIMENSION statement which had originally declared the matrices was then deleted as redundant, since

the common blocks DIMV and ADTNL now handled that function.

EQUIVALENCE(INDXPT,I1)

This statement was corrected by replacing I1 through I4 with INDXPT(1) through INDXPT(4), respectively. This involved extensive modification of equations in the AREA, IDOUT, and SFORCE subroutines. In particular, the IDOUT subroutine presented problems in statement numbers IDOT 187 and IDOT 262. In those lines, there are implied DO loops in the WRITE statements. The index value, II, of each of the DO loops is bounded by the initial value I1 and the test value I4. These needed to be replaced by INDXPT(1) and INDXPT(4), but the array locations could not be used in the implied DO loop as the initial and test values. Instead, the addition of the following two statements immediately preceding the affected WRITE statements resolved the problem:

IPIGZ=INDXPT(1)

IDAWGZ=INDXPT(4)

These two integer-valued variables were then inserted into each WRITE statement implied DO loop as the initial and test values, respectively.

EQUIVALENCE(XGP,THG),(YGP,PHIG)

This pair of statements had to be corrected by replacement, since all of the listed variables are 21 x 21 size matrices and a listing of the equivalence of each location would have been too lengthy. After checking all of the listings of the individual variables, the logical replacement choice was to replace THG and PHIG by XGP and YGP, respectively. This was decided because there were many new equations with XGP and YGP, and the fact that, although THG and PHIG were listed in all the INPT common blocks, all the common block replacements could be



made with one command due to the unique listing of the variables, separated by commas, which is found only in the common blocks and other deceleration statements. Therefore, using the WYLBUR terminal, one CHANGE command eliminated most of the locations of THG and PHIG.

The only other location where THG and PHIG were listed was in the BLOCK DATA section of the program, where simple substitution in the Hollerith string was made. This same line was included as one of the BLOCK DATA errors covered later in this appendix.

In conclusion, the variable matrices THG and PHIG were replaced by XGP and YGP, which involved a simple substitution in the INPT common block and one line in the BLOCK DATA section of the HVOSM.

```
EQUIVALENCE(YPNO,P)
```

```
EQUIVALENCE(YNO,Q)
```

YPNO and YNO were two one-dimensional arrays, 30 addresses long. These variables were all confined to the PINT1 subroutine, and YPNO and YNO were the least used pair of variables out of each pair of possible variable choices. Since there were so few references to YPNO and YNO in the subroutine, it was a simple matter to replace them with P and Q, respectively. Both EQUIVALENCE statements were deleted, and YPNO and YNO had to be deleted from a DIMENSION statement and a DOUBLE PRECISION statement in the PINT1 subroutine to complete this correction.

```
EQUIVALENCE(HCAH,HCAH1),(HCBH,HCBH1),(HCGH,HCGH1)
```

This EQUIVALENCE statement was corrected in a different way from all of the previous ones. There were considerable numbers of each variable in the program, so that no clear choice presented itself as in the other EQUIVALENCE statements. Also, this EQUIVALENCE statement, along with the arrays HCAH, HCBH, and HCGH only occurred in the VGORNT

subroutine. Since this statement only caused an error in one subroutine, and since each array was only a one-dimensional, four location array, the solution used in this case was to list each location in each array to an equivalent variable. Therefore, the EQUIVALENCE statement was enlarged so that each of the four locations in the arrays HCAH, HCBH, and HCGH were linked to the variables HCAH1 through HCAH4, HCBH1 through HCBH4, and HCGH1 through HCGH4, respectively. As previously stated, this was a unique case because of the great number of listings of each variable in the program and the fact that this substitution only had to be performed in the VGORNT subroutine.

#### BLOCK DATA Errors

There were three simple errors in the BLOCK DATA section of the program, all of which were easily corrected and which are mentioned as a timesaver in case the corrections need to be made again.

First of all, in line BDAT 7, there was a closure of the data set listing before the array was filled. The BAX data set was defined as 30 locations long, but the string ran out after 22 places were filled. Therefore, at the end of the string, eight spaces had to be filled as follows:

,8\* ' '/

This will fill up the remaining eight spaces in the array and then eliminate the error message.

The second error was almost identical to the first. The BEX array was also defined as 30 locations long, but the data listed only 21 spaces before it ended. Therefore, the following was added after the last parenthetical listing:

'9\*' '/'

This added the required nine spaces to the string to complete the array and eliminate the error message.

The final BLOCK DATA error message was due to Hollerith string errors. The original listing, in part, was shown in subroutine IDOUT as:

```
DATA IDDATA/12HZPG,THG,PHIG/,---
```

The mistake here is that three variables have been defined in one Hollerith string, with the commas included. As mentioned in the EQUIVALENCE error portion, THG and PHIG were replaced by XPG and YPG, respectively, so the correct listing ends up as:

```
DATA IDDATA/3HZPG,3HXPG,3HYPG/,---
```

APPENDIX IV  
PROGRAM MODIFICATION LISTING

This additional section lists the computer printouts of the changes made to the HVOSM in order to add the sign impact option, along with the regular program statements surrounding each modified area so that the precise location of the changes in the HVOSM can be found.

Figure 35 is a listing of the changes made to the main program. While it does not include the placement of COLL, SUBB, or NUMT in the common blocks, that was explained sufficiently well that it was not required. As the last variable in the BARRIER common block, the ERASE statement had to be changed also to clear COLL and SUBB along with the rest of the common block by inserting SUBB(7,50) in the place of the second argument in the parameter list for that program statement.

Figure 36, covering three pages, illustrates the changes made to the INPUT subroutine, while Figure 37 illustrates the two additions made to the SFORCE subroutine at the beginning and end of the subroutine. Finally, Figure 38 lists the formats and variable lists used to identify and arrange the printout of the SUBB matrix in the IDOUT subroutine.

```

COMPUTED TO IT=IT+1 AFTER RETURNING FROM SVAPLT, WHICH ALLOWS OPEN ENDEMAIN 113
CONCERNING DATA SETS AND SEQUENTIAL DATA SETS PER JOB FOR PRIVATE PAK MAIN 114
      IT=8
      MAIN 115
CET      NPTS FOR NUMBER OF WRITES = NUMBER POINTS/CATEGORY(MAIN TO PLTP)MAIN 116
C*****
C*** THE COMMON/BARRIER/ BLOCK HAS BEEN MODIFIED FOR THE SIGN IMPACT *****
C*** VERSION OF THIS PROGRAM BY THE ADDITION OF THE 'COLL' TRIGGER *****
C*** OPTION VALUE AND THE 'SUBB(7,50)' MATRIX OF IMPACT FORCES AND *****
C*** THEIR LOCATIONS WITH TIME. THE COMMAND BELOW THIS CLEARS THE *****
C*** VALUE OF 'COLL' FOR LATER IN THE PROGRAM. THE COMMON/INPT1/ *****
C*** BLOCK HAS BEEN MODIFIED BY THE ADDITION OF THE 'NUNT' VARIABLE *****
C*** WHICH WILL BE USED TO INDICATE THE NUMBER OF TIME POINTS USED *****
C*** TO READ IN THE IMPACT FORCES AND LOCATIONS. IT IS ALSO CLEARED *****
C*** TO A VALUE OF ZERO BELOW AT THE START OF THE PROGRAM. *****
C*****
      NUNT=0
      NPTS=1
      BEX(30)=0.
1 CALL ERASE(PH10,PQRMIN)
  CALL ERASE(YCIP(1),PSIFD0)
      MAIN 117
      MAIN 118
      MAIN 119
      MAIN 120

```

Figure 35. Modification of MAIN Program.

```

DATA SAVE/'SAVE'/                               INPT 114
DATA FINI/'FINI'/                               INPT 115
DATA STN /'STAN'/                               INPT 116
DATA TNONE /'NONE'/                             INPT 117
NSAVE=0                                          INPT 118
C*****
C*** THIS IS PART OF THE SIGN IMPACT MODIFICATION FOR THE CURRENT *****
C*** HVOSH USING AN IMPACT MATRIX OF THE FORCES AND LOCATIONS WITH TIME *****
C*** THE NEXT LINE CLEARS A VARIABLE USED TO LOAD THE MATRIX FROM *****
C*** THE INPUT DATA *****
C*****
JJ=0
IAPFR(1) = 0                                    INPT 119
IAPFR(2) = 0                                    INPT 120
JUT=0                                           INPT 121
ALPHA=0.0                                       INPT 122

2 READ 1001, (CARDIM(K),K=1,20),(DUM(I),I=1,9),ICARD          INPT 133
1001 FORMAT( 20A4,11,9F8.0,I8)                                INPT 134
WRITE(6,1011) (CARDIM(K),K=1,20)                              INPT 135
1011 FORMAT( 1X,20A4)                                         INPT 136
IF(ICARD.EE.9999) GOTO 60                                     INPT 137
C*****
C*** THE 'GO TO' OPTIONS LISTED BELOW HAS BEEN MODIFIED BY THE ADDITION *****
C*** OF THE LABEL 53 FOR WHEN ICARD EQUALS 29, TO READ IN THE IMPACT *****
C*** FORCES AND LOCATIONS WITH TIME AS MODIFIED BY JOHN BETZ *****
C*****
60 TO (3,4,5,6,7,8,9,10,11,12,13,14,15,16,19,20,21,22,23,24,26,32,INPT 138
1 34,35,36,37,38,39,53),ICARD                                INPT 139
WRITE(6,2001) (CARDIM(K),K=1,20)                              INPT 140

```

Figure 36. Modification of INPUT Subroutine.

```

EM = DUM(3)                                INPT 223
AAA = DUM(4)                                INPT 224
HMAX = DUM(5)                               INPT 225
HAIN = DUM(6)                               INPT 226
BET = DUM(7)                                INPT 227
C*****
C*** THIS IS PART OF THE VEHICLE IMPACT MODIFICATION PERFORMED ON THE *****
C*** PROGRAM. THE VARIABLE 'COLL' HAS BEEN ADDED AS A SIGNAL USED *****
C*** LATER IN THE SFORCE SUBROUTINE TO PREVENT THE BARRIER OPTION *****
C*** FROM COMING INTO PLAY WITHOUT AVOIDING THE REST OF THE PROGRAM. *****
C*** THIS ALSO ALLOWS THE BARRIER OPTION TO BE KEPT AND THEREFORE THE *****
C*** PROGRAM IS AVAILABLE FOR A VARIETY OF PROBLEMS. THE OTHER *****
C*** VARIABLE, 'NUMT', IS THE READ-IN VALUE OF THE NUMBER OF *****
C*** DISCRETE TIME STEPS WHICH WILL BE READ INTO THE PROGRAM TO *****
C*** REPRESENT THE IMPACT FORCES AND LOCATIONS FOR THE SIMULATION. *****
C*** THE VALUE OF 'NUMT' MUST BE BETWEEN 1 AND 50, AND IT SHOULD *****
C*** INCLUDE A ZERO TIME VALUE, THE FINAL TIME VALUE WHEN ALL THE *****
C*** FORCES ARE ZERO, AND THE TIME POINT IN THE FUTURE WHICH WILL KEEP *****
C*** THE FORCES ZEROED OUT FOR THE PROGRAM AS IT KEEPS RUNNING. THE *****
C*** THE LAST TIME POINT SHOULD BE A LONG PERIOD BETWEEN THE NEXT-TO- *****
C*** LAST SO THE PROGRAM CAN RUN THE VEHICLE REACTION. *****
C*****
COLL=DUM(8)
NUMT=DUM(9)
GO TO 2                                     INPT 228
5 XAS = DUM(1)                               INPT 229
XAF = DUM(2)                                INPT 230
XAR = DUM(3)                                INPT 231

```

Figure 36. (continued)

```

XSTI(J)=XSTI0(J)                                INPT 521
YSTI(J)=YSTI0(J)                                INPT 522
391 ZSTI(J)=ZSTI0(J)                             INPT 523
      GOT02                                       INPT 524
C*****
C*** THIS PART OF THE SUBROUTINE LOADS THE FORCES AND LOCATIONS DUE *****
C*** TO IMPACTS WITH TIME INTO THE 'SUBB' MATRIX, WHICH IS CAPABLE *****
C*** OF 50 DISCRETE TIME INPUT VALUES. THE MATRIX SIZE AS DEFINED *****
C*** IN THE COMMON/BARRIER/ BLOCK IS (7,50). THE SEVEN POSITIONS AS *****
C*** THEY ARE USED IN THIS MODIFICATION ARE AS FOLLOWS: *****
C*** 1. THIS IS THE TIME LOCATION *****
C*** 2. THIS IS THE IMPACT FORCE ALIGNED IN THE LOCAL VEHICLE *****
C*** X-AXIS DIRECTION, POSITIVE OR NEGATIVE *****
C*** 3. THIS IS THE IMPACT FORCE ALIGNED IN THE LOCAL VEHICLE *****
C*** Y-AXIS DIRECTION, POSITIVE OR NEGATIVE *****
C*** 4. THIS IS THE IMPACT FORCE ALIGNED IN THE LOCAL VEHICLE *****
C*** Z-AXIS DIRECTION, POSITIVE OR NEGATIVE *****
C*** 5. THIS IS THE X LOCATION OF THE FORCES FROM THE MASS CENTER *****
C*** OF THE VEHICLE, POSITIVE OR NEGATIVE *****
C*** 6. THIS IS THE Y LOCATION OF THE FORCES FROM THE MASS CENTER *****
C*** OF THE VEHICLE, POSITIVE OR NEGATIVE *****
C*** 7. THIS IS THE Z LOCATION OF THE FORCES FROM THE MASS CENTER *****
C*** OF THE VEHICLE, POSITIVE OR NEGATIVE *****
C*** JJ IS JUST A COUNTER TO LOAD THE MATRIX *****
C*****
53 JJ=JJ+1
   SUBB(1,JJ)=DUM(1)
   SUBB(2,JJ)=DUM(2)
   SUBB(3,JJ)=DUM(3)
   SUBB(4,JJ)=DUM(4)
   SUBB(5,JJ)=DUM(5)
   SUBB(6,JJ)=DUM(6)
   SUBB(7,JJ)=DUM(7)
   GO TO 2
   END
C SINGLE VEHICLE ACCIDENT SIMULATION WITH CURB IMPACT - CRBIMP          INPT 525
CRAP -1

```

Figure 36. (continued)



```

NSLCE = 0
NUMLD=0
NUMLD2=0
YBIVF = 0.0
SFOR 111
SFOR 112
SFOR 113
SFOR 114
C*****
C*** THIS IS PART OF THE SIGN IMPACT MODIFICATION AS MADE BY JOHN BETZ *****
C*** TO THE EXISTING MVOSA PROGRAM. THE FOLLOWING COMMAND WILL MAKE *****
C*** THE PROGRAM FLOW SKIP ALL THE PROVISIONS OF THIS PROGRAM AND *****
C*** DIRECTLY FIND THE IMPACT FORCES AND MOMENTS AS FOUND IN THE *****
C*** MATRIX 'SUBB'. THE LINEAR INTERPOLATION METHOD WILL BE USED *****
C*** LATER IN THIS SUBROUTINE TO FIND THOSE FORCES AND MOMENTS AT ANY *****
C*** TIME INTERVAL. THE FORCES AND MOMENTS ARE LOADED INTO THE *****
C*** PROGRAM NAMES OF 'SFXS', 'SFYS', 'SFZS', AND 'SNPS', 'SNTS', 'SNPSS', *****
C*** RESPECTIVELY. THAT IS IN THE ORDER OF X, Y, AND Z. *****
C*****
IF(COLL.EQ.1.) GO TO 1002
IF(INDB.EQ.0) RETURN
IB = (INDB+1)/2
2 00 3 1=1,3
SFOR 115
SFOR 116
SFOR 117

1000 FURMAT(F7.4,2F7.1,5I3,12F8.1)
NLDCR = NLDCR+1
RETURN
SFOR 470
SFOR 471
SFOR 472
C*****
C*** THIS IS WHERE THE PROGRAM GOES TO USE THE IMPACT FORCES AND *****
C*** LOCATIONS TO FIND THE FORCES AND MOMENTS TO USE FOR THE CAR MOTION *****
C*** EQUATIONS. THIS USES LINEAR INTERPOLATION AND OUTPUTS THE FORCES *****
C*** AND MOMENTS TO USE IN THE MATRIX SUBROUTINE. *****
C*****
1002 I=2
1003 IF(T.LE.SUBB(1,I)) GO TO 1004
I=I+1
GO TO 1003
1004 IM1=I-1
VART=(T-SUBB(1,IM1))/(SUBB(1,I)-SUBB(1,IM1))
SFXS=SUBB(2,IM1)+VART*(SUBB(2,I)-SUBB(2,IM1))
SFYS=SUBB(3,IM1)+VART*(SUBB(3,I)-SUBB(3,IM1))
SFZS=SUBB(4,IM1)+VART*(SUBB(4,I)-SUBB(4,IM1))
ECKS=SUBB(5,IM1)+VART*(SUBB(5,I)-SUBB(5,IM1))
WHY= SUBB(6,IM1)+VART*(SUBB(6,I)-SUBB(6,IM1))
ZEE= SUBB(7,IM1)+VART*(SUBB(7,I)-SUBB(7,IM1))
SNPS=SFZS*WHY-SFYS*ZEE
SNTS=SFXS*ZEE-SFZS*ECKS
SNPSS=SFYS*ECKS-SFXS*WHY
RETURN
END
SFOR 473
C
VGRN -1
C
SINGLE VEHICLE ACCIDENT SIMULATION WITH CURB IMPACT - VGRNT
VGRN 0

```

Figure 37. Modification of the SFORCE Subroutine.

```

WRITE(6,2028) APF,APR                                IDOUT 340
2028 FORMAT(49H0ANT1-PITCH TABLES FOR CIRCUMFERENTIAL TIRE FORCE /, IDOUT 341
1 5H APF= , 11F10.3/ , 5X,10F10.3/,5H APR=, 11F10.3/,5X,10F10.3) IDOUT 342
C*****
C*** THIS IS PART OF THE SIGN IMPACT MODIFICATION TO THE EXISTING *****
C*** HVOSM PROGRAM AS MADE BY JOHN BETZ. THE FOLLOWING COMMANDS *****
C*** PRINT OUT THE IMPACT FORCES AND LOCATIONS AS READ IN IN THE *****
C*** INPUT SUBROUTINE. THE FORCES ARE IN POUNDS, THE DISTANCES ARE *****
C*** IN INCHES, AND THE TIME IS IN SECONDS. THIS ALSO USES THE 'COLL' *****
C*** TRIGGER TO INDICATE WHETHER THE IMPACT PART OF THE PROGRAM IS *****
C*** IN EFFECT. *****
C*****
IF(COLL.NE.1.) GO TO 1020
PRINT 1030
1030 FORMAT('-', 'SIGN IMPACT FORCE AND LOCATION DATA ***** **
1 *****')
PRINT 1035
1035 FORMAT('0', 'TIME (SEC)', 5X, 'X FORCE(LB)', 5X, 'Y FORCE(LB)',
15X, 'Z FORCE(LB)', 7X, 'X (IN)', 9X, 'Y (IN)', 9X, 'Z (IN)')
DO 1037 I=1,NUMT
PRINT 1036, SUBB(1,I), SUBB(2,I), SUBB(3,I), SUBB(4,I), SUBB(5,I)
1, SUBB(6,I), SUBB(7,I)
1036 FORMAT(' ', F10.3, 6X, F10.3, 6X, F10.3, 6X, F10.3, 5X, F10.3, 5X, F10.3,
15X, F10.3)
1037 CONTINUE
1020 CONTINUE
CALL BRIVID                                IDOUT 343
WRITE (6,1007)                                IDOUT 344
1007 FORMAT (1H1)                                IDOUT 345
RETURN                                IDOUT 346

```

Figure 38. Modification of the IDOUT Subroutine.

## VITA

Author's name: John Frederick Betz

PII Redacted

Father's name: Frederick A. Betz

Mother's name: Barbara A. Betz

EDUCATION: B.S. degree in May, 1978, from U.S. Air Force Academy  
Double major in Civil Engineering and Engineering Mechanics  
Commissioned 2nd Lt. in USAF on May 31, 1978  
Outstanding Cadet in Military Science  
Outstanding Cadet in Civil Engineering  
Outstanding Cadet in Engineering Mechanics  
Graduated 22 out of 978

Area of Specialty: Structural analysis

The typist for this thesis was Mrs. Sylvia Velasco.